POLYETHYLENE GLYCOL STATIONARY PHASES FOR CAPILLARY GAS CHROMATOGRAPHY

by

Kelly A. Turner

Thesis submitted to the Faculty of the
Virginia Polytechnic Institute and State University
in partial fulfillment of the requirements for the degree of

MASTER OF SCIENCE

in

Chemistry

APPROVED:

H.M. McNair, Chairman

L.T. Taylor

J. Mason

September, 1988

Blacksburg, Virginia

POLYETHYLENE GLYCOL STATIONARY PHASES FOR CAPILLARY GAS CHROMATOGRAPHY

by

Kelly A. Turner

Committee Chairman: Harold M. McNair
Chemistry

(ABSTRACT)

The chromatographic properties of various silicone stationary phases for capillary gas chromatography have been extensively studied, yet the properties of nonsilicone phases have not been so well investigated. The most popular nonsilicone phases are the high molecular weight polyethylene glycols (HMW PEG) which are commercially available in a wide range of molecular weights, cross-linkable and uncross-linkable (Carbowax 20M and 40M, the Superox series, etc.). Their most outstanding features are their unique polarity and selectivity; for this reason these phases are widely used in the analysis of aqueous solutions, essential oils, and perfumes.

Unfortunately HMW-PEG's are very sensitive to slight differences in preparation and handling procedures which can cause analyses to differ with each laboratory, each column, and even each use. HMW-PEG's also suffer from low

temperature stability, a high minimum allowable operating temperature, and have lower diffusion coefficients than silicone phases.

This study examines the efficiency differences of eight columns differing only in immobilization procedure and added functional groups. Comparison is made using HETP versus u and separation number (TZ) versus u curves. These curves offer important information, in particular, the effect of carrier gas, u, column operating temperature, degree of cross-linking, and cross-linking temperature on chromatographic efficiency and separation number. In addition, the contributions of the C_L (resistance to mass transfer in the liquid phase) and D_L (diffusion coefficient in the liquid phase) terms in the Golay equation are calculated [1].

Solids at room temperature, PEG stationary phases undergo a solid-liquid phase transition within their useful temperature range. The effect of this transition on the chromatographic properties is investigated using efficiency, separation number, capacity ratio, and retention index versus temperature curves. Four more columns, in addition to the eight mentioned above, demonstrate the influence of end-groups and the molecular weight of the stationary phase on the phase transition temperature range.

ACKNOWLEDGEMENTS

I would like to thank and of the Research Institute for Chromatography, in Wevelgem, Belgium, without whose dedicated help and concern this work would not have been possible. I would also like to thank them and their families as well as , , and and their families for their hospitality and making my stay in Belgium such a wonderful experience. Thanks is also due to my research director, Dr. Harold McNair, his help and for arranging my study in Belgium. In addition I would like to express my appreciation to his secretary and my good friend, , for her help and thoughtfulness over the years.

For all of his understanding, support, and encouragement, especially in this last year, I would like to thank my fiance, . I hope to always be as supportive of him as he has been of me.

I would also like to express my extreme gratitude toward my parents. They have been understanding and encouraging and always been there when I needed them.

A very large thanks is also in order to everyone at J & W Scientific who were there for help and support in the

final effort to finish this work, especially

, , and .

TABLE OF CONTENTS

ABSTRACT ii

ACKNOWLEDGEMENTS iv

INTRODUCTION 1

Resolution Optimization in CGC 1

Polyethylene Glycols as CGC Stationary Phases . . 5

Cross-linking of Polyethylene Glycols 14

EXPERIMENTAL 16

RESULTS AND DISCUSSION 22

Physical Properties of Stationary Phases 22

Chromatographic Evaluation 26

CONCLUSION 67

VITA 70

REFERENCES 68

LIST OF FIGURES

Figure 1a. Differential scanning calorimetric analysis of commercial, auto-crosslinkable PEG. 23

Figure 1b. Differential scanning calorimetric analysis of commercial Superox. 23

Figure 2a. Thermogravimetric analysis of commercial, autocross-linkable PEG. 25

Figure 2b. Thermogravimetric analysis of commercial Superox. 25

Figure 3a. HETP v. u curves for NXL column at 30°C using hydrogen, nitrogen, and carbon dioxide carrier gases. Comparison is made to SOX with nitrogen carrier gas. Analyte = dodecane. 29

Figure 3b. HETP v. u curves for NXL column at 70°C using hydrogen, nitrogen, and carbon dioxide carrier gases. Comparison is made to SOX with nitrogen carrier gas. Analyte = tridecane. . . . 29

Figure 4a. HETP v. u curves for XL-150 column at 30°C using hydrogen, nitrogen, and carbon dioxide carrier gases. Comparison is made to SOX with nitrogen carrier gas. Analyte = dodecane. 30

Figure 4b. HETP v. u curves for XL-150 column at 70°C

using hydrogen, nitrogen, and carbon dioxide carrier gases. Comparison is made to SOX with nitrogen carrier gas. Analyte = tridecane. . . . 30

Figure 5a. HETP v. u curves for PEG phase columns at 30°C with nitrogen carrier gas. Analyte = dodecane. 32

Figure 5b. HETP v. u curves for PEG phase columns at 70°C with nitrogen carrier gas. Analyte = tridecane. 32

Figure 6a. HETP v. u curves for FFAP phase columns at 30°C with nitrogen carrier gas. Analyte = dodecane. 33

Figure 6b. HETP v. u curves for FFAP phase columns at 70°C with nitrogen carrier gas. Analyte = tridecane. 33

Figure 7. HETP v. u curves for PEG phase columns at 70°C with nitrogen carrier gas. Analyte = butanol. 39

Figure 8a. N/m v. Temperature curves for the uncross-linked columns (NXL and SOX) using nitrogen carrier gas. Comparison is made to two cross-linked columns (XL-150 and XL-200). Analyte = undecane. 40

Figure 8b. N/m v. Temperature curves for the cross-linked PEG columns using nitrogen carrier gas. Analyte = undecane. 40

Figure 9a. N/m v. Temperature curves for the uncross-linked NXL column using nitrogen carrier gas. Comparison is made to two cross-linked columns (XL-150 and XL-200). Analyte = butanol. 43

Figure 9b. N/m v. Temperature curves for the cross-linked PEG columns using nitrogen carrier gas. Analyte = butanol. 43

Figure 10a. N/m v. Temperature curve for the Commercial-II column using nitrogen carrier gas. . 44

Figure 10b. N/n v. Temperature curves for the Commercial-I, HM-2500, and HM-10,000 columns. Nitrogen carrier gas was used for the two HM columns and hydrogen was used for Commercial-I. . 44

Figure 11a. TZ v. u curves for separation of n-dodecane and n-tridecane on the autocross-linkable PEG phases using nitrogen carrier gas at 70°C. . . 47

Figure 11b. TZ v. u curves for separation of 2-pentanol and 1-butanol on the autocross-linkable PEG phases using nitrogen carrier gas at 70°C. . . 47

Figure 12a. TZ v. Temperature curves for the uncross-

linked columns (NXL and SOX) using nitrogen carrier gas. Comparison is made to two cross-linked columns (XL-150 and XL-200). Analytes = decane and undecane. 48

Figure 12b. TZ v. Temperature curves for the cross-linked PEG columns using nitrogen carrier gas. Analytes = decane and undecane. 48

Figure 13a. TZ v. Temperature curves for the uncross-linked NXL column using nitrogen carrier gas. Comparison is made to two cross-linked columns (XL-150 and XL-200). Analytes = propanol and butanol. 49

Figure 13b. TZ v. Temperature curves for the cross-linked PEG columns using nitrogen carrier gas. Analytes = propanol and butanol. 49

Figure 14a. k v. Temperture curves for the uncross-linked columns (NXL and SOX) using nitrogen carrier gas. Comparison is made to two cross-linked columns (XL-150 and XL-200). Analyte = undecane. 51

Figure 14b. k v. Temperture curves for the cross-linked PEG columns using nitrogen carrier gas. Analyte = undecane. 51

Figure 14c. k v. Temperature curves for the Commercial-I, HM-2500, and HM-10,000 columns. Nitrogen carrier gas was used for the two HM columns and hydrogen was used for Commercial-I. . 52

Figure 15. k and N v. Time at 30°C. 54

Figure 16. Five chromatographic analyses of C_9-C_{12} hydrocarbons under identical conditions (hydrogen carrier gas at u=33 cm/s, 45°C isothermal. 56

Figure 17a. RI v. Temperature curves for propanol on the autocross-linkable PEG phases using nitrogen carrier gas. 58

Figure 17b. RI v. Temperature curves for propanol on the cross-linked PEG phases using nitrogen carrier gas. 58

Figure 18a. Retention indices fo McReynolds compounds at 30°C using hydrogen, nitrogen, and carbon dioxide carrier gases. 63

Figure 18b. Retention indices fo McReynolds compounds at 70°C using hydrogen, nitrogen, and carbon dioxide carrier gases. 63

Figure 19a. Retention indices of McReynolds compounds at 30°C and 70°C on NXL and SOX columns using nitrogen carrier gas. 64

Figure 19b. Retention indices of McReynolds compounds at 30°C and 70°C on XL-150 and Xl-200 columns using nitrogen carrier gas. 64

Figure 19c. Retention indices of McReynolds compounds at 30°C and 70°C on XL-250 and XL-250-AO columns using nitrogen carrier gas. 65

Figure 19d. Retention indices of McReynolds compounds at 30°C and 70°C on Commercial-I using nitrogen carrier gas. 65

LIST OF TABLES

Table 1. Unit structures of two polyethylene glycol stationary phases and modifiers. 17

Table 2. Column Description 19

Table 3. Experimental Diffusion Coefficients. 37

Table 4. Retention Indices of McReynolds Compounds on Various Columns. 61

INTRODUCTION

Resolution Optimization in CGC

In gas chromatography, the most important factor influencing resolution is the selectivity of the chromatographic system. For a given sample, selectivity is determined by the choice of the stationary phase. This is a well known fact in packed column GC where the most suitable stationary phase can be thoughtfully chosen from more than 300 commercially available stationary phases.

However, capillary columns have much higher plate numbers which allows many separation problems to be solved by "brute" efficiency using a capillary column coated with an apolar dimethylsilicone stationary phase. Only recently has the importance of selectivity in capillary gas chromatography been emphasized. The growing interest in selectivity optimization has prompted further developments in stationary phase synthesis and reinvestigation of selectivity tuning specifically for capillary columns.

In gas chromatography, the resolution of two compounds is expressed by the master resolution equation:

$$R = \left(\frac{\sqrt{N}}{4}\right)\left(\frac{\alpha-1}{\alpha}\right)\left(\frac{k_2}{k_2+1}\right) \qquad (1)$$

where

N = the plate number of the column which is dependent on the length of the column, L, and the height equivalent to a theoretical plate (HETP), h as shown below:

$$N = \frac{L}{h} \quad \text{and} \tag{2}$$

$$N = 5.545 \left(\frac{t_R}{w_{1/2}}\right)^2 \tag{3}$$

where $w_{1/2}$ is peak width at half-height.

α = the selectivity factor which depends on the relative retention of two compounds:

$$\alpha = \frac{t'_{R(2)}}{t'_{R(1)}} = \frac{k_2}{k_1} \tag{4}$$

where t'_R is the adjusted retention time (peak retention time - retention time of a nonsorbed peak, t_m)

k = the capacity factor which is dependent on the distribution coefficient, K, and on the phase ratio, β (β = volume of mobile phase / volume of

stationary phase):

$$k = \frac{K}{\beta} = \frac{t'_R}{t_m} \qquad (5)$$

High resolution capillary gas chromatography is the result of optimization of the three contributions, column efficiency, selectivity and capacity ratio. For years chromatographers related the resolving power of a capillary column almost exclusively to its plate number while hardly considering optimization of the selectivity and capacity ratio for the separation at hand. Insufficient separation of peaks of interest was remedied by using longer columns to increase plate numbers; however the result was a slight resolution enhancement at the expense of a proportional increase in analysis time.

An alternative to increasing plate number through column length is to reduce the HETP value. The height equivalent to a theoretical plate expresses the rate of band broadening, or efficiency, in capillary columns and is described by the Golay equation [1]:

$$HETP = \frac{2D_G}{u} + \frac{(1+6k+11k^2)r^2}{24(1+k)^2 D_G} u + \frac{2}{3} \frac{k}{(1+k)^2} \frac{d_f^2}{D_L} u \qquad (6)$$

where:

D_G is the diffusion coefficient in the gas phase,

D_L is the diffusion coefficient in the liquid phase,

r is the internal column radius, and

d_f is the stationary phase film thickness.

In practice, the internal column radius has the greatest influence on efficiency. The minimum HETP value is reduced proportionally with internal diameter reduction. Consequently long, narrow bore columns (internal diameter < 100um) can give extremely high plate counts (more than 1,000,000); however, compared to a separation on a standard capillary column (25m x 0.25mm i.d.), the higher plate number only has a small influence on resolution [2]. In addition, long, narrow bore columns suffer limitations such as high inlet pressure requirements and long analysis times.

Recently, there has been an interest in resolution optimization through adjusting capacity factor. Compounds having a low capacity factor ($k < 2$) require very high plate counts for separation. As an example, two compounds having $k_1 = 0.49$ and $k_2 = 0.50$ and therefore $\alpha = 1.02$, require 375,000 theoretical plates to achieve the minimum resolution ($R = 1$). But if the capacity ratios are increased by a factor of 5, the number of plates required is reduced to 81,500. Stationary phase film thickness has the largest

influence on k, though column operating temperature and the nature of the stationary phase itself also play a role. For this reason, the analysis of very volatile compounds by capillary gas chromatography (CGC) was made possible with the introduction of thick film columns. However the capacity factor has limited influence on resolution; increasing the capacity factor by increasing film thickness or lowering column operating temperature will only give a considerable resolution increase for compounds with $k < 2$.

Finally, the greatest resolution enhancement results from optimizing the selectivity of the chromatographic system. Selectivity is a more complex parameter than plate number or capacity; it is dependent on all interactions between the stationary phase and the analytes. The chemical structures of the stationary phase and solutes and the column operating temperature greatly influence these interactions. For this reason stationary phase choice is critical and is therefore the starting point in selectivity optimization.

Polyethylene Glycols as CGC Stationary Phases

A large variety of stationary phases have been used in packed column GC. However capillary GC has been very

limited in the use of stationary phases; the highly inert glass and fused silica surfaces possess a very low surface energy and therefore polar liquid phases do not wet the surface, instead, droplet formation occurs. For this reason stationary phase selection in high resolution CGC should be based primarily on criteria other than selectivity. A summary of these criteria are as follows:

1. The stationary phase must coat the smooth capillary surface efficiently without surface roughening techniques such as $BaCO_3$, NaCl deposition, and whiskers. Partial destruction of the inert glass or silica surface, low coating efficiencies compared to dimethylsilicone phases, and lower thermal stability of the phase after coating due to catalytic decomposition by the inorganic layer are some of the disadvantages to these treatments [3].
2. High purity of the stationary phase is necessary to avoid decomposition of the phase due to catalytic activity of residual impurities and to ensure column inertness.
3. The phase must have high thermal stability and a

wide useful temperature range.

4. Ideally, the stationary phase should allow for immobilization without the incorporation of cross-linking agents and without negatively affecting the chromatographic properties.

For the above reasons the apolar dimethyl silicones are far superior to any of the other stationary phases. Dimethyl silicone phases produce highly efficient columns; the smooth, homogeneous coating of the capillary surface is due to the low surface tension and gum character of these phases. By definition, a gum is a linear, high molecular weight polymer that is a solid at room temperature and still soluble in organic solvents. In addition, the viscosity of the phase is only minimally influenced by temperature, ensuring high thermostability of the phase.

In the case of the more polar phases, only high molecular weight polyethylene glycols (HMW-PEG) have been used with any relative degree of success. Other polar phases used in packed column GC have low viscosities and are high surface tension liquids at GC temperatures; therefore they cannot be coated efficiently on the highly inert, smooth surfaces. The reason polyethylene glycol phases coat so well is not completely understood, but is most likely due

to their being high viscosity, gum phases. HMW-PEG, specifically Carbowax 20M (molecular weight = 20,000), made the transition from packed to capillary GC because, unlike many of the other polar phases, they can be coated efficiently on smooth fused silica and glass without surface roughening.

The high capability for hydrogen bonding gives the HMW-PEG's a unique polarity and selectivity; therefore they are considered to be one of the five basic capillary GC phases [3][4]. Because of the problems encountered so far with nonsilicone stationary phases, Stark et al.[4] suggested the substitution of a silicone containing 40-45% cyanopropyl and 20-25% phenyl for polyethylene glycol. This was tested by Sandra et al.[3] using two techniques; first, by the mixing of two commercial phases, RSL-300 (50% methyl, 50% phenyl) and RSL-1000 (90% biscyanopropyl, 10% methylvinyl), to produce a mixed phase (45% cyanopropyl, 25% phenyl, and 30% methyl groups), and second by direct series coupling of RSL-300 and RSL-1000 columns. They found that by combining these silicone phases, the polarity of HMW-PEG can be obtained. Unfortunately, PEG's unique selectivity could not be duplicated.

HMW-PEG phases have many problems associated with them

[5]. They have relatively low temperature stability; for example, Carbowax 20M coated on bare fused silica is only stable to 180°C. Above this temperature droplet formation occurs. On a column pretreated with NaCl or $BaCO_3$, the temperature stability is elevated to 220°C, and if a whisker layer is deposited before coating, the upper temperature limit is 240°C. Another drawback to the HMW-PEG phases is the minimum allowable operating temperature (MiAOT) of 55°C.

Carbowax phases are very sensitive to oxygen and water. Relatively high concentrations of metal ions catalyze phase degradation. This phase also has a relatively low molecular weight and suffers from batch to batch variability. PEG's also have lower diffusion coefficients than silicone phases and are also very sensitive to small differences in preparation and handling procedures which causes nonuniform results between columns and between analyses; this causes difficulties in interlaboratory exchange of retention data.

The introduction of the Superox phases helped eliminate some of these problems [6][7][8]. The purity of these phases is much higher than for Carbowax phases. After preparation, the polymer is ultra centrifuged to reduce metal contamination. These phases can be synthesized in much higher molecular weights, up to 5,000,000, than

Carbowax phases and are linear. The configuration of Carbowax 20M is not known exactly and is believed to have nonlinear chains. Another advantage of Superox phases is the elevated maximum allowable operating temperature (MAOT) of 250°C. Superox also produces columns with higher coating efficiencies than Carbowax (>95% versus 75-80%); in other words, columns with 20% higher plate numbers can be attained. This efficiency enhancement is due to the gum phase nature of Superox. The polarity of Superox is only slightly lower than that of Carbowax.

Nevertheless, HMW-Superox still suffers some disadvantages. The phase has an alkaline character. The peak area ratio for dimethyl phenol (DMP) : dimethyl aniline (DMA), as described by Grob [9], obtained on Superox columns is less than one. This implies the irreversible adsorption of acids. The high molecular weight Superox phases possess a very high viscosity and form a gel when dissolved for coating. For example, Superox 0.1 columns can only be coated using a high pressure liquid chromatography pump. Superox 0.1 has a molecular weight of 100,000 and an MAOT approximately 20°C lower than Superox 4 (MW = 4,000,000).

An alternative to these very high molecular weight phases is Superox 20M (MW=20,000) which is also a linear

molecule and can be synthesized by treating Superox 0.1 with hydrochloric acid. It is a pure, white powder with high solubility -- solutions of 15 - 20% are possible. This lower molecular weight phase has an MAOT of 220°C when coated on bare fused silica and 250°C on a rough, treated surface. This phase has a much lower calcium ion (Ca^{+2}) concentration than Superox 4, but its MAOT is lower than that of Superox 4. However this is not due to the low metal ion concentration since addition of Ca^{+2} to the phase has no effect on phase stability. Another advantage of Superox 20M is the satisfactory DMA : DMP peak area ratio.

Superox 20M can also be used to produce a tuned phase suitable for the analysis of free fatty acids. This free fatty acid phase (FFAP) is the result of melting Superox 20M together with 2-nitroterephthalic acid. This tuned phase has a higher MAOT of 250°C.

Many different procedures for immobilizing polyethylene glycol films have been investigated and immobilization degrees of 100% are attainable, but all procedures give a film with increased activity compared to pure polyethylene glycol coatings [6][10]. In addition, Cramers et al. [11] found no significant difference between conventionally coated and in situ cross-linked stationary silicone phases,

specifically, between CP-Sil-5 and CP-Sil-5-CB and between OV-1 and OV-1-CB. For PEG phases, on the other hand, this is not the case. For bondable PEG, cross-linking temperature and column operating temperature both play a role in the overall efficiency of a column.

The specific analytical need at hand dictates whether an immobilized or nonimmobilized film must be applied. For instance, an immobilized film must be used in the analysis of aqueous solutions, whereas for the analysis of essential oils and perfumes, a normal PEG is best. Advertisements by commercial companies for immobilized polyethylene glycol columns also show less than perfect inertness by the adsorption of nonanal and by the DMA : DMP peak area ratio not being equal to one for the Grob test mixture.

How cross-linking chromatographically affects the PEG phase is addressed in this paper. Replicate, isothermal injections of hydrocarbons were made on the different PEG columns. Retention times and efficiencies were calculated at different temperatures with different carrier gases and even at different equilibration times.

From a chromatographic viewpoint, PEG stationary phases undergo a solid-liquid phase transition within their useful temperature range. When operating the column below the

melting point of the stationary phase, compounds are separated on the basis of adsorption as in gas-solid chromatography. When operating above the melting point, compounds are separated through partitioning since gas-liquid chromatography is being applied.

HETP versus u curves are plotted at 30°C and 70°C for various PEG phase columns to compare the efficiency of a separation based on adsorption to one based on partitioning. The columns used are identical in dimensions, but they differ in immobilization procedure and added functional groups. In each case, the efficiency of each PEG phase varies drastically between the adsorption and partitioning modes. The nonimmobolized PEG columns show the greatest efficiency enhancement in going from the adsorption to the partitioning mode.

How a column's chromatographic properties are affected across the solid-liquid transition range are investigated through efficiency, capacity ratio, separation number (TZ), and retention index (RI) versus temperature curves. TZ and RI were calculated from the following equations:

$$TZ = (t_{r,b} - t_{r,a})/(w_{1/2,a} + w_{1/2,b}) - 1 \qquad (7)$$

where the subscripts a and b denote two compounds in an homologous series.

$$RI = 100n_a + (\log t_r - \log t_{r,a})/(\log t_{r,b} - \log t_{r,a}) \quad (8)$$

where n denotes the carbon number of the previous hydrocarbon and the subscripts a and b denote the previous and following hydrocarbons respectively.

Six curves were generated for seven columns manufactured in-house using a commercially available autocross-linkable PEG of molecular weight 20,000. In addition curves were generated for five more columns coated with PEG phases from different commercial suppliers so that the impact of cross-linking and molecular weight on transition range could be studied.

Cross-linking of Polyethylene Glycols

The aim of cross-linking stationary phases is to produce a column which: (1) has better film stability; (2) shows no or low bleed at elevated temperatures; (3) suffers no phase stripping with on-column injection or large solvent injection; and (4) is rinsable upon contamination. Immobilization of carbowax, a PEG stationary phase, was

first introduced by Aue and Hastings [12]. The immobilization was carried out by a high temperature (280°C) polycondensation reaction between the PEG phase and the glass capillary surface. Since then, many variations of this method and new methods for PEG immobilization have been documented [13-25].

The exact method used for the immobilization of the autocross-linkable phase mentioned above is not available since this is a commercial phase, yet it is known to contain a cross-linking agent -- most likely epichlorohydrin. Since this paper addresses the chromatographic differences between cross-linked and uncross-linked stationary phases, a lengthy discussion and understanding of the exact cross-linking method is not necessary. We only need to note the differences in chromatographic behavior between an immobilized and non-immobilized phase.

EXPERIMENTAL

Three commercially available PEG stationary phases, each having molecular weights of 20,000, were used for investigation and comparison: 1) Superox 20M, a PEG phase comparable to Carbowax 20M; 2) an autocross-linkable PEG phase; and 3) a free fatty acid phase (FFAP), a "tuned", autocross-linkable PEG phase for the analysis of free fatty acids. **Table 1** shows the structure and differing features of each of these phases. Superox, the simplest, is a straight chain PEG polymer. The autocross-linkable phase is a PEG with a cross-linking agent, most likely epichlorohydrin, introduced. The FFAP phase is synthesized by melting 2-nitroterephthalic acid together with a PEG phase before adding a cross-linking agent.

To investigate the polymers' physical properties Thermogravimetric (TGA) and Differential Scanning Calorimetric (DSC) analyses were run on the Superox and commercial PEG phases.

For chromatographic evaluation of the columns, a Hewlett-Packard model HP-5890 gas chromatograph and a Spectra Physics model SP-2340 integrator were used.

Column preparation was standardized for capillary columns 25m long with a 0.25mm internal diameter (i.d.), and

Table 1. Unit structures of two polyethylene glycol stationary phases and modifiers.

	Structure	Use
PEG unit	$HO-[CH_2CH_2O]_n-H$	stationary phase
epichlorohydrin	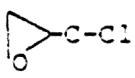	crosslinking agent - free radical generator
FFAP unit	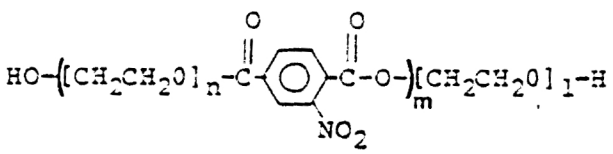	stationary phase - a tuned PEG phase for the analysis of free fatty acids. Synthesized by melting 2-nitroterephthalic acid with PEG.
2-nitrotereph-thalic acid	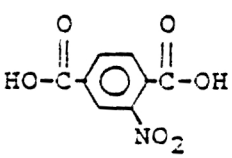	phase modifier

a 0.5um stationary film thickness (d_f). After rinsing with dichloromethane, the 25m lengths of fused silica tubing were dried under nitrogen flow and statically coated with a 7.84 mg/cc solution of PEG in dichloromethane giving a film thickness of 0.5um. The freshly prepared columns were then conditioned and/or cross-linked in different manners as shown in **Table 2**. Four other columns were also used for comparison. Commercial-I and Commercial-II were purchased columns with chemically bonded PEG stationary phases. HM-2500 and HM-10,000 were columns coated with homemade stationary phases synthesized in-house from PEG units with molecular weights of 2500 and 10,000 respectively. These four phases also differ from the other PEG's in the fact that they are end-capped with tri-ethoxy-siloxanes which allow in-column immobilization. See **Tables 1** and **2** for phase structures and column descriptions.

Each column's efficiency was tested both as a function of average linear carrier gas velocity (u) and temperature. Nitrogen was used as carrier gas for all these tests except for the Commercial-I column case, in which hydrogen was used. The effect of carrier gas was studied using hydrogen, nitrogen and carbon dioxide carrier gases. Efficiency as a

TABLE 2. Column Description

COLUMN NAME	DIMENSIONS	STATIONARY PHASE	IMMOBILIZATION
SOX	25m x 0.25mm ID x 0.5um df	SUPEROX 20M MW=20,000	UNCROSSLINKED, CONDITIONED AT 100°C FOR 2 HOURS
UXL	25m x 0.25mm ID x 0.5um df	AUTOCROSSLINKABLE, COMMERCIAL PEG PHASE, MW=20,000	UNCROSSLINKED, CONDITIONED AT 100°C FOR 1 HOUR
XL-150	25m x 0.25mm ID x 0.5um df	AUTOCROSSLINKABLE, COMMERCIAL PEG PHASE, MW=20,000	CONDITIONED AT 100°C FOR 1 HOUR, CROSSLINKED AT 150°C FOR 3 HOURS (UXL AFTER CROSSLINKING)
XL-200	25m x 0.25mm ID x 0.5um df	AUTOCROSSLINKABLE, COMMERCIAL PEG PHASE, MW=20,000	CROSSLINKED AT 200°C FOR 8 HOURS
XL-250	25m x 0.25mm ID x 0.5um df	AUTOCROSSLINKABLE, COMMERCIAL PEG PHASE, MW=20,000	CROSSLINKED AT 250°C FOR 8 HOURS
XL-250-AO	25m x 0.25mm ID x 0.5um df	AUTOCROSSLINKABLE, COMMERCIAL PEG PHASE + 5% IRGANOX 1073, MW=20,000	CROSSLINKED AT 250°C FOR 8 HOURS
FFAP-200	25m x 0.25mm ID x 0.5um df	AUTOCROSSLINKABLE, COMMERCIAL FFAP PHASE, MW=20,000	CROSSLINKED AT 200°C FOR 8 HOURS
FFAP-250	25m x 0.25mm ID x 0.5um df	AUTOCROSSLINKABLE, COMMERCIAL FFAP PHASE, MW=20,000	CROSSLINKED AT 250°C FOR 8 HOURS
COMM-I	15m x 0.32mm ID x 0.5um df	PURCHASED COLUMN, PEG PHASE	CHEMICALLY BONDED
COMM-II	25m x 0.33mm ID x 1.3um df	PURCHASED COLUMN, PEG PHASE	CHEMICALLY BONDED
HM-2500	10m x 0.25mm ID x 0.2um df	HOMEMADE PHASE FROM PEG UNITS MW=2500	CROSSLINKED
HM-10,000	15m x 0.32mm ID x 0.25um df	HOMEMADE PHASE FROM PEG UNITS MW=10,000	CROSSLINKED

function of u was studied by constructing Height Equivalent to a Theoretical Plate (HETP) versus u curves at 30°C and 70°C. 1uL injections of alkanes and alcohols in hexane (1ug/uL, split ratio 1:100) were made at increasing carrier gas velocities. Methane was also drawn into the loaded syringe to provide a dead time (t_m) reference. HETP and u were then calculated from the following equations:

$$HETP = L/N = L/5.545\ (t_r\ /w_{1/2})^2 \qquad (9)$$

$$u = L/t_m \qquad (10)$$

where L is column length, t_r is peak retention time, and $w_{1/2}$ is peak width at half height.

The diffusion coefficient in the liquid phase, D_L, was calculated for each column from the experimental HETP versus u curves using the following data and the Golay equation as described by Sandra et al.[26] : $D_G = 0.1\ cm^2/s$ for nitrogen, r = 0.0125 cm, and $d_f = 0.5x10^{-4}$ cm.

Efficiency as a function of temperature was investigated through number of plates per meter (N/m) versus T curves. Alkanes and alcohols were injected as above at 5°C intervals from 25°C to 90°C while column head pressure

remained constant. N/m was calculated:

$$N/m = N/L. \quad (11)$$

The separation numbers (TZ), for alkanes and alcohols were also calculated and plotted as a function of u and T for each column using equation 7. Retention indices (RI) of alcohols relative to hydrocarbons were calculated and graphed as a function of T using equation 8. Capacity ratios (k) of alkanes and alcohols were calculated and graphed as functions of T from the following equation:

$$k = (t_r - t_m)/t_m \quad (12)$$

The selectivity of each of the columns was tested by calculating the RI's of the McReynolds compounds at 30°C and 70°C. The components tested were the n-alkanes (C_8 to C_{13}), benzene, pyridine, butanol, 2-methyl-2-pentanol, nitropropane, 1-iodobutane, 2-octyne, 1,4-dioxane, and cis-hydrindane.

RESULTS AND DISCUSSION

Physical Properties of Stationary Phases

1) DSC of Superox and PEG

As a preliminary experiment a DSC (differential scanning calorimetric) analysis was made of the commercial stationary phase. **Figures 1a** and **1b** show the scans of the commercial PEG and Superox respectively. In **Figure 1a**, the transition point for the first heating (H1), the cooling (C), and the second heating (H2) are not the same. The first heating has the highest temperature transition, 60°C, and has a shoulder at the base of the peak which is most likely due to the reaction of the cross-linking agent since this phase and the Superox phase differ only in the presence of the cross-linking agent and this shoulder is not present in the scan of the Superox polymer (**Figure 1b**). The cooling transition occurs much lower at 34°C. The transition for the second heating is slightly lower and more narrow than for the first heating, and has no shoulder. This suggests that the cross-linking agent reacts with the polymer during the first heating, altering the polymer molecular structure between the two cycles. A slightly higher transition is seen for the Superox relative to the commercial PEG in

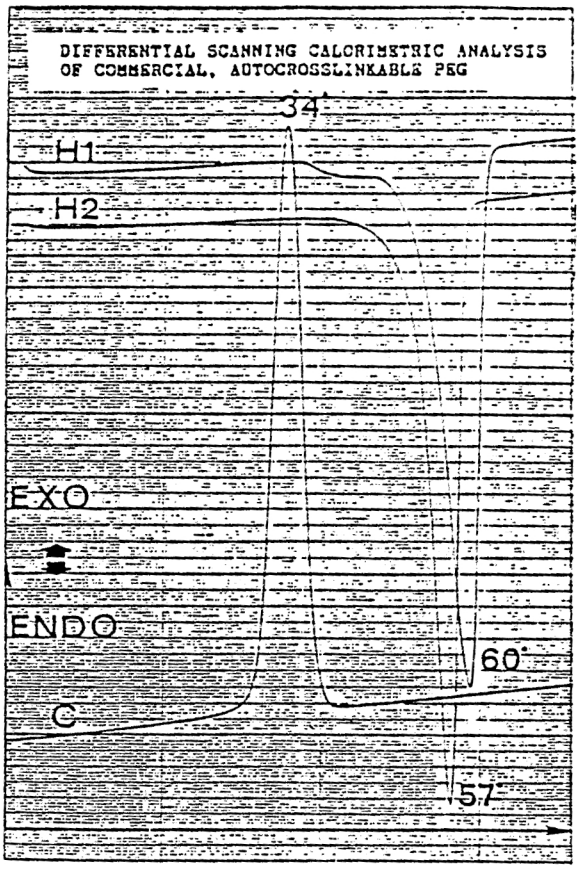

Figure 1a. Differential scanning calorimetric analysis of commercial, autocrosslinkable PEG. Heating rate = 10 C/min.

Figure 1b. Differential scanning calorimetric analysis of commercial Superox. Heating rate = 10 C/min.

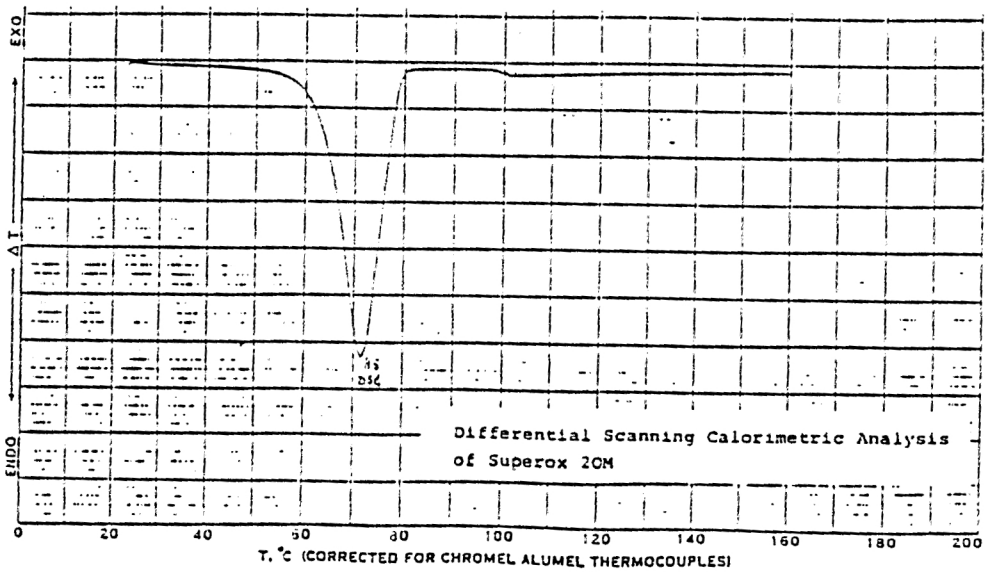

Figure 1b. A possible explanation for the difference in transition temperatures between H1, C, and H2 is a combination of two factors: cross-linking, and thermal lag.

The fast heating and cooling rates of the scans (10°C/min) do not allow the polymer to achieve its lowest energy state at each point; consequently, this appears as a reduced transition temperature upon cooling. For this reason the data should be viewed relatively instead of absolutely.

Secondly, the PEG changes significantly when cross-linked. The end groups and the cross-linking agent react to form bridges between the polymer chains resulting in a continuous network of the phase as opposed to separate chains with reactive end groups. Since the cross-linking partially destroys the crystallinity of the phase, a lower transition point is observed. In addition, this more homogeneous phase displays a more narrow transition range.

2) TGA of Superox 20M, PEG, and FFAP

Figures 2a and **2b** are Thermogravimetric Analysis (TGA) scans of the autocrosslinkable PEG and Superox phases, respectively. The scan for the autocross-linkable

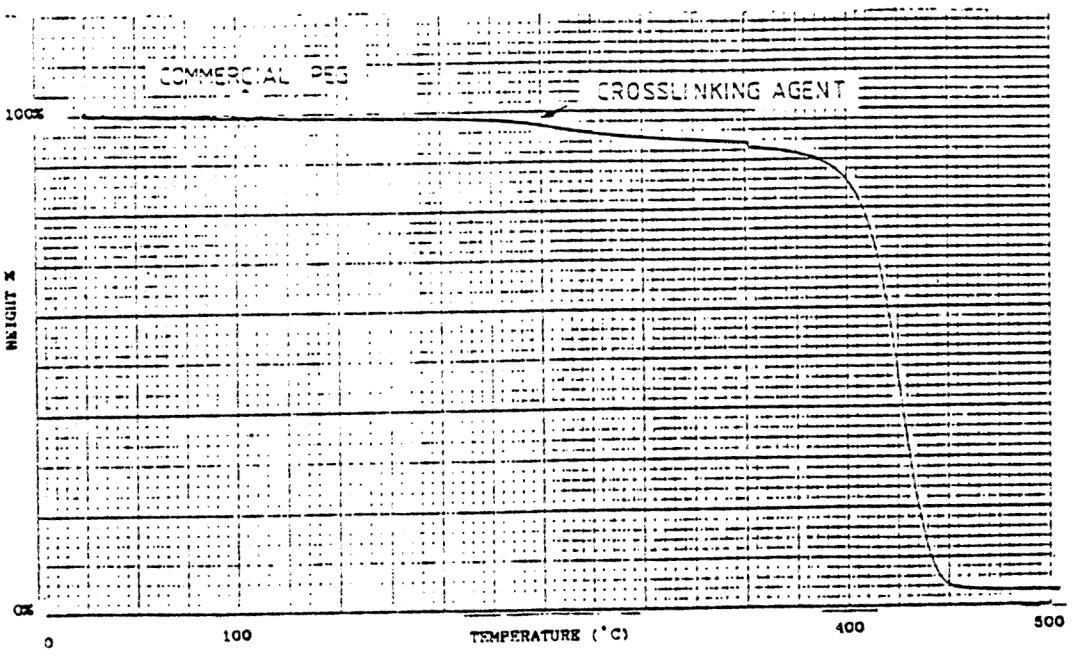

Figure 2a. Thermogravimetric analysis of commercial, autocrosslinkable PEG.

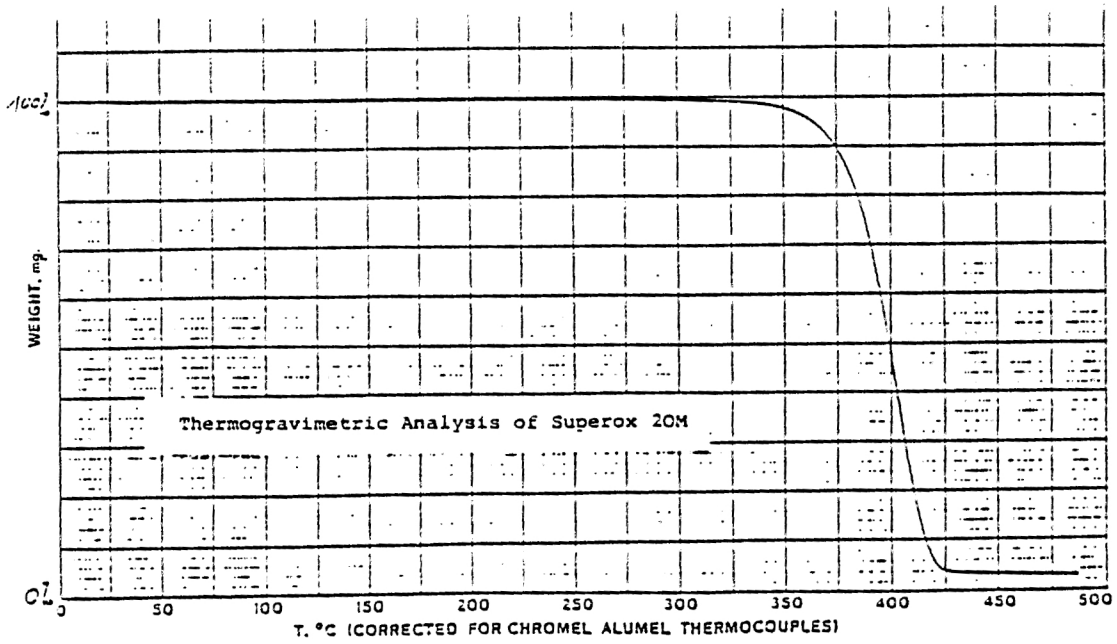

Figure 2b. Thermogravimetric analysis of commercial Superox.

PEG shows an earlier, more pronounced decrease than the Superox. This again must indicate the reaction of the cross-linking agent, as in the DSC scan above, since this is the only difference between the two phases.

Chromatographic Evaluation

The three factors contributing to a column's overall resolution are efficiency, selectivity, and capacity. Each column's resolution was investigated by measuring each of these contributing factors. By injecting a series of alkanes and alcohols while first varying carrier gas velocity and then temperature, the three contributions could be studied as a function of u and T.

Efficiency

Rate of band broadening in capillary columns is described by the Golay equation (1). At very high carrier gas velocity, the first term of the three term equation can be ignored and the expression written:

$$h = C_G u + C_L u \qquad (13)$$

where C_G is the resistance to mass transfer in the gas phase and C_L is the resistance to mass transfer in the liquid

phase.

The slope of the HETP versus u curve can then be set equal to (C_G + C_L) at very large u values; C_G can be calculated from the values given above, thereby allowing C_L to be found. For two columns of identical dimensions (length, i.d., d_f) differing only in stationary phase and tested under identical conditions (temperature, carrier gas, linear gas velocity), the only difference in HETP versus u curves will be a difference in slope due to a difference in diffusion coefficients. In other words, the more efficient column -- the one with less band broadening -- will have the smaller slope and greater D_L. D_L can be calculated from C_L, k, and d_f.

Being solids at room temperature, PEG stationary phases undergo a solid-liquid phase transition within their useful temperature range (see DSC scans, **Figure 1**). When operating the column below the melting point of the stationary phase, compounds are separated on the basis of adsorption; when operating above the melting point, compounds are separated through partitioning.

HETP versus u curves were plotted to study the effect of column operating temperature, choice of carrier gas, and cross-linking temperature on efficiency.

The HETP versus u curves in **Figures 3a** and **3b** were generated from the analysis of dodecane and tridecane at 30°C and 70°C, respectively, on the SOX and NXL columns (see **Table 2** for abbreviated column names and descriptions). For simplicity, error bars are shown only for the NXL column using nitrogen carrier gas, since the standard deviation was nearly constant between columns and carrier gases at a given temperature. **Figures 4a** and **4b** are analogous for the XL-150 column. To investigate the effect of carrier gas, NXL and XL-150 were evaluated using hydrogen, nitrogen and carbon dioxide. Since the diffusion coefficient of a gas, D_G, is inversely proportional to the square root of its molecular weight, the order of carrier gas efficiency, according to the Golay equation, should be: hydrogen > nitrogen > carbon dioxide. This order is confirmed in **figures 3b, 4a** and **4b**, but the NXL column at 30°C, **figure 3a**, shows best efficiency with carbon dioxide. No reasonable explanation for this phenomenon is known. Because this effect is observed only on the NXL and not the XL-150 column, it must be due to an

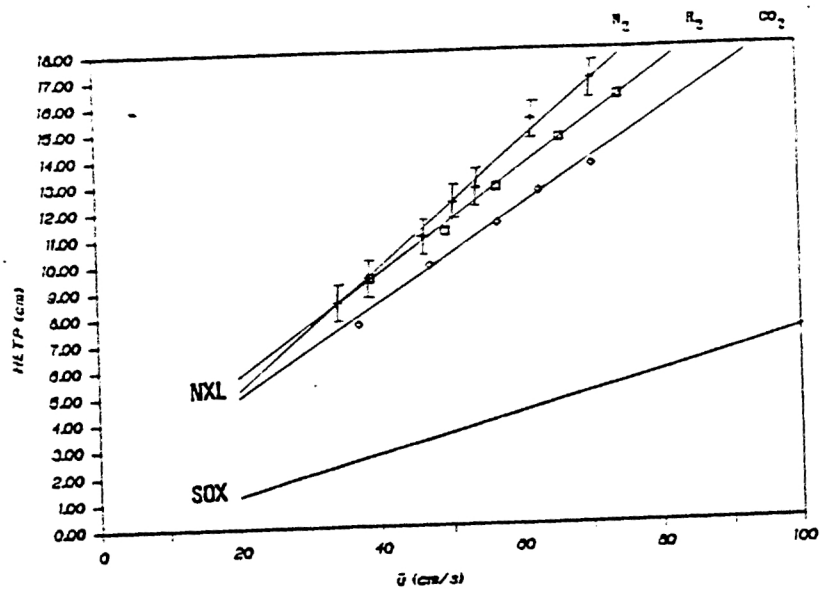

Figure 3a. HETP v. u curves for NXL column at 30°C using hydrogen, nitrogen, and carbon dioxide carrier gases. Comparison is made to SOX with nitrogen carrier gas. Analyte = dodecane.

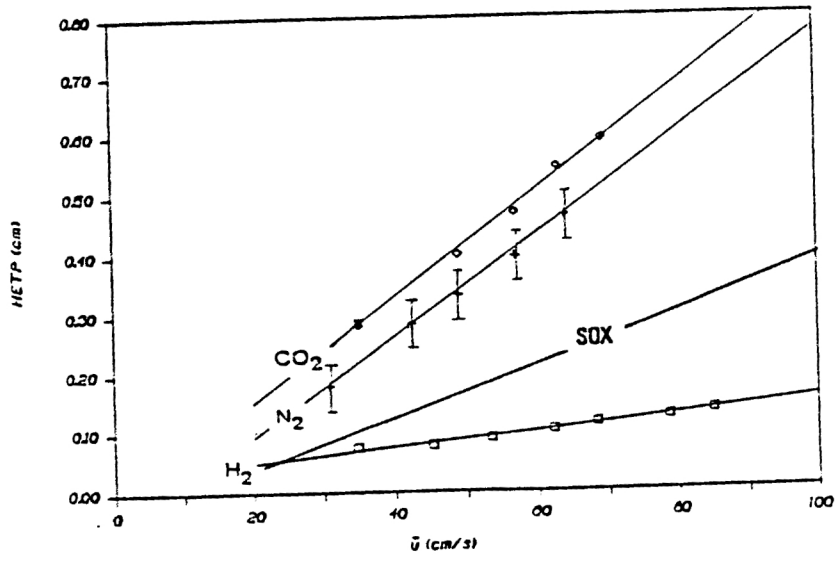

Figure 3b. HETP v. u curves for NXL column at 70°C using hydrogen, nitrogen, and carbon dioxide carrier gases. Comparison is made to SOX with nitrogen carrier gas. Analyte = tridecane.

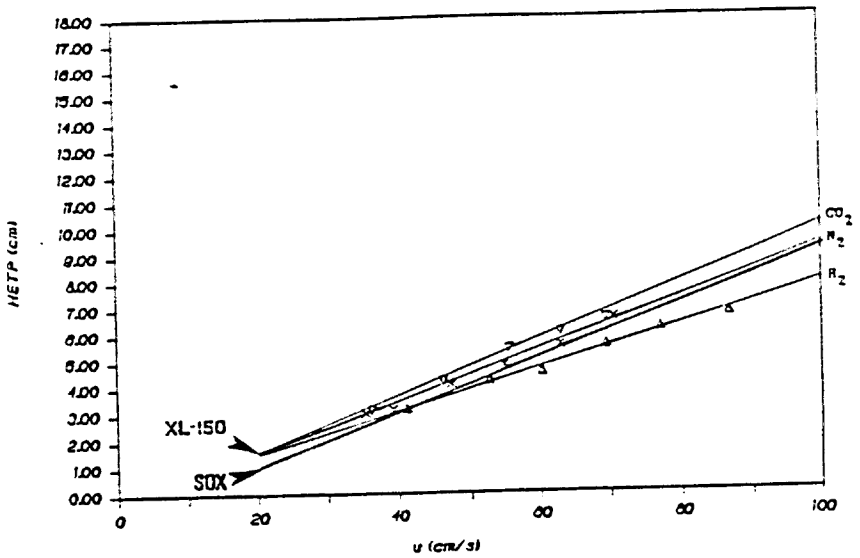

Figure 4a. HETP v. u curves for XL-150 column at 30°C using hydrogen, nitrogen, and carbon dioxide carrier gases. Comparison is made to SOX with nitrogen carrier gas. Analyte = dodecane.

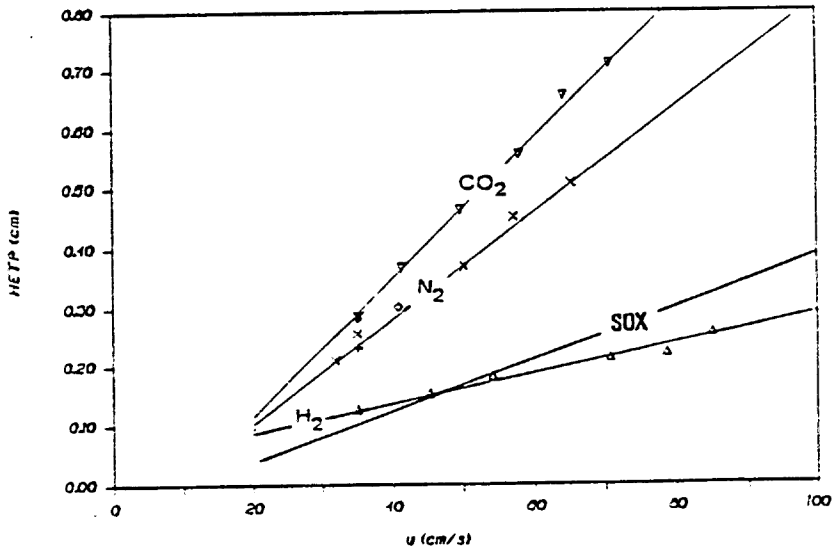

Figure 4b. HETP v. u curves for XL-150 column at 70°C using hydrogen, nitrogen, and carbon dioxide carrier gases. Comparison is made to SOX with nitrogen carrier gas. Analyte = tridecane.

interaction of the uncross-linked stationary phase and the carbon dioxide at 30°C and is not just a carrier gas effect.

The SOX column at 30°C shows an efficiency between that of NXL and XL-150, but at 70°C SOX shows the highest overall efficiency. The efficiency of SOX is much greater than the efficiency of NXL, due either to the intrinsic nature of the phase or the absence of the cross-linking agent.

The difference between a separation based on adsorption and one based on partitioning can be seen by comparing the HETP versus u curves at 30°C to those at 70°C. In going from the adsorption to the partitioning mode, a large efficiency increase is observed for all three columns; SOX, NXL, and XL-150. **Figures 5a** and **5b** demonstrate this behavior for all of the PEG phase columns: SOX, NXL, XL-150, XL-200, XL-250, XL-250-AO. **Figures 6a** and **6b** show the same effect for FFAP-200 and FFAP-250.

How cross-linking temperature affects efficiency in the adsorption mode can be seen by comparing **Figures 5a** and **6a.** At 30°C the order of increasing efficiency is: NXL < XL-150 < SOX < XL-250 $\cong$ XL-250-AO < XL-200 < FFAP-250 $\leq$ FFAP-200. Looking only at the autocross-linkable PEG phase series (NXL, XL-150, XL-200, XL-250, XL-250-AO), cross-linking

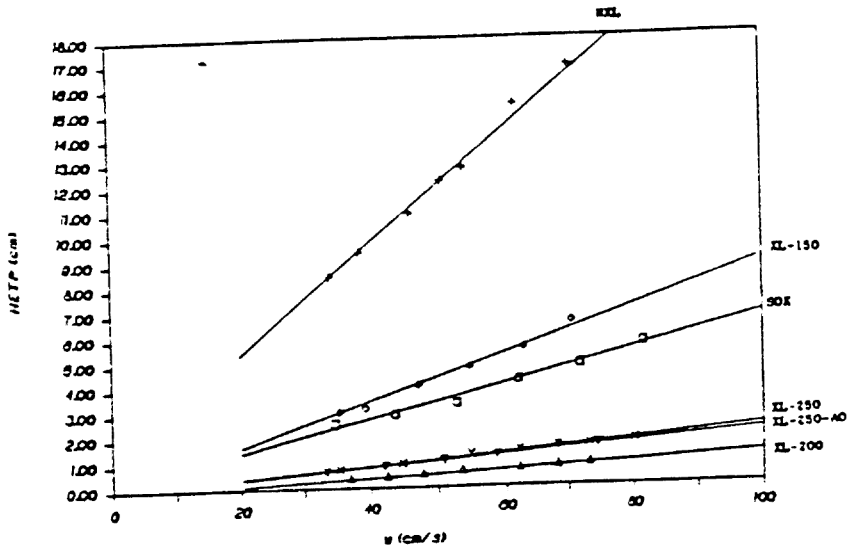

Figure 5a. HETP v. u curves for PEG phase columns at 30°C with nitrogen carrier gas. Analyte = dodecane.

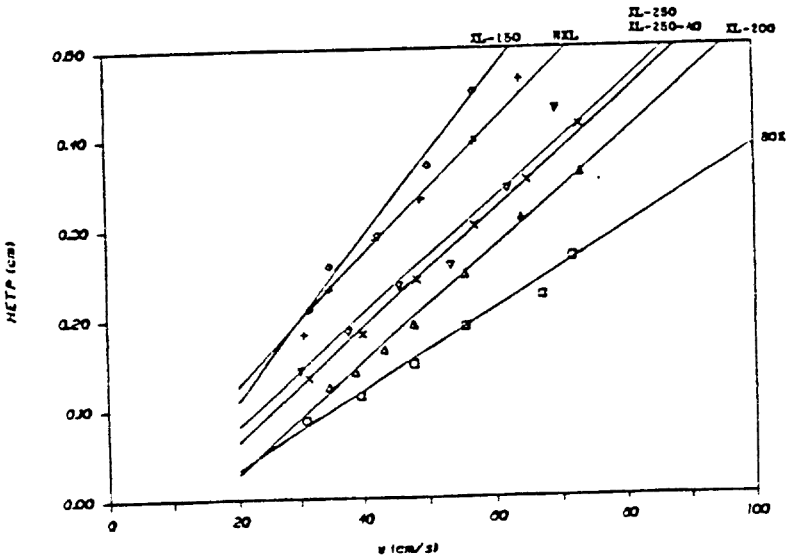

Figure 5b. HETP v. u curves for PEG phase columns at 70°C with nitrogen carrier gas. Analyte = tridecane.

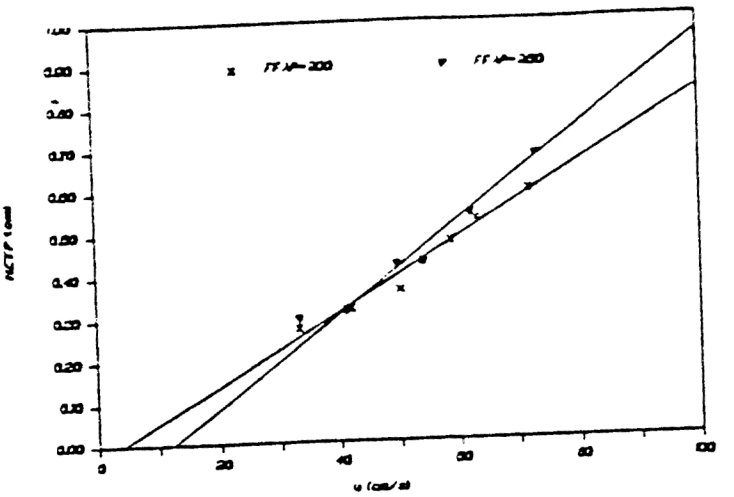

Figure 6a. HETP v. u curves for FFAP phase columns at 30°C with nitrogen carrier gas. Analyte = dodecane.

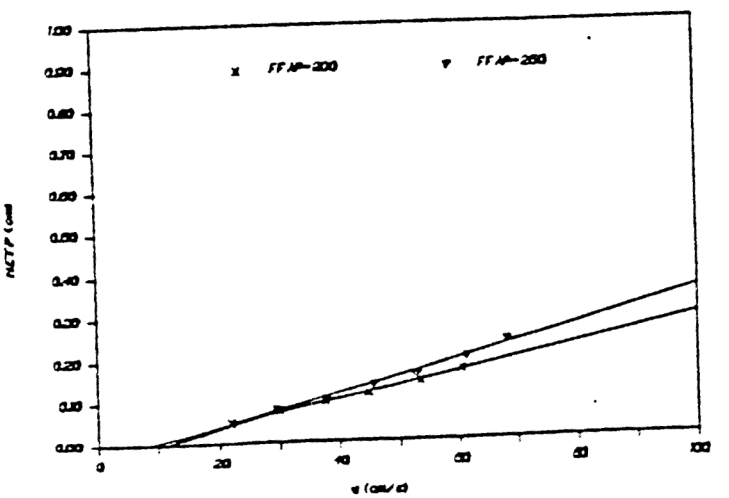

Figure 6b. HETP v. u curves for FFAP phase columns at 70°C with nitrogen carrier gas. Analyte = tridecane.

enhances efficiency and the optimum cross-linking temperature is 200°C -- above this temperature efficiency is lost.

Though they show greater overall efficiency, the same is observed but to a much lesser degree for the two FFAP phases; 200°C is the optimum cross-linking temperature. Since the functional group incorporated into the FFAP phase for selectivity tuning gives the phase a more acidic character, a possible explanation for the better efficiency is a more homogeneous coating of the acidic fused silica surface. In the partitioning mode, **Figures 5b** and **6b**, the order of increasing efficiency of the phases is: XL-150 < NXL < XL-250-AO ≅ XL-250 < XL-200 < SOX ≅ FFAP-250 < FFAP-200. There are two major differences from the adsorption mode; NXL becomes more efficient than XL-150, and SOX shows efficiency comparable to the FFAP phases. In other words the efficiency shift going from the adsorption to the partitioning mode for uncross-linked columns is much greater than that for cross-linked columns. This follows the assumption made above that uncross-linked phases are more crystalline than cross-linked phases in the adsorption mode -- cross-linking partially destroys crystallinity. In the partitioning mode, the difference in efficiencies of the

columns is not as great as in the adsorption mode; therefore the shift in efficiency going from 30°C to 70°C for the uncross-linked phases is more pronounced. Most importantly, the most efficient strictly PEG phase in the partitioning mode is SOX, an uncross-linked phase, whereas in the adsorption mode the most efficient phase is the one cross-linked at the optimum temperature of 200°C.

In both partitioning and adsorption modes NXL and XL-150 show the lowest efficiencies for the cross-linkable PEG's. Recall that XL-150 is actually NXL after cross-linking; this column was first conditioned at 100°C for 2 hours, tested as NXL, then cross-linked and retested as XL-150. The low efficiency of this column may be due to unreacted or partially reacted cross-linking agent or the low conditioning and cross-linking temperatures.

The conditioning method used to cross-link the bondable PEG plays an important role in its efficiency. Although cross-linking begins about 140°C, conditioning is usually carried out at 200°C or above. It is possible that cross-linking at 140-150°C can produce a "bubbled" film possibly due to trapped carrier gas during cross-linking. For a bondable PEG at 150°C, the viscosity may not be low enough to allow the vapors to completely escape. In addition, the

onset of cross-linking may be causing still a further increase in viscosity. The product is a column with a bubbled coating having much lower efficiency than a column conditioned at a higher temperature for a longer time period.

The average k, slope of the HETP versus u curve, C_G, C_L, and D_L were calculated for each of the columns above at both temperatures and are given in **Table 3.** In addition the ratio $D_L(30°C):D_L(70°C)$ is calclated. The ratio of the D_L value of each column at 30°C and 70°C is compared to that of SOX at 30°C and 70°C respectively to compare the diffusivity of the commercial, autocross-linkable liquid phase to that of the uncross-linked Superox phase under the same conditions. Because the method used for calculating D_L is only a approximation, the absolute values of these coefficients should not be examined, but rather the general trends examined and compared. These values reconfirm the conclusions drawn above. Efficiency curves were also constructed at 70°C using an alcohol instead of an alkane to investigate the effect of solute. These curves

Table 3. Experimental Diffusion Coefficients.

COLUMN	Temperature (C)	TEST COMPONENT	k(avg)	SLOPE of NITROGEN h v.u curve	CG (s)	CL (s)	DL (cm/s)	RATIO of DL 30C : 70C	RATIO DL : DL(SOX)
SOX	70	TRIDECANE	10.58	0.0041	6.2910E-04	3.4709E-03	3.7886E-08	0.06	----
	30	DODECANE	9.32	0.0671	6.1888E-04	6.6481E-02	2.1938E-09		----
NXL	70	TRIDECANE	9.63	0.0078	6.2164E-04	7.1704E-03	1.9780E-08	0.03	0.52
	30	DODECANE	9.80	0.2349	6.2304E-04	2.3428E-01	5.9777E-10		0.27
XL-150	70	TRIDECANE	9.29	0.0091	6.1864E-04	8.4814E-03	1.7235E-08	0.08	0.45
	30	DODECANE	10.93	0.0972	6.3154E-04	9.6568E-02	1.3259E-09		0.60
XL-200	70	TRIDECANE	8.26	0.0064	6.0821E-04	5.7918E-03	2.7720E-08	0.32	0.73
	30	DODECANE	12.76	0.0134	6.4251E-04	1.2757E-02	8.8043E-09		4.01
XL-250	70	TRIDECANE	8.42	0.0075	6.0997E-04	6.8900E-03	2.2953E-08	0.23	0.61
	30	DODECANE	11.94	0.0233	6.3798E-04	2.2662E-02	5.2443E-09		2.39
XL-250 AO	70	TRIDECANE	8.61	0.0070	6.1198E-04	6.3880E-03	2.4324E-08	0.19	0.64
	30	DODECANE	13.26	0.0241	6.4502E-04	2.3455E-02	4.6336E-09		2.11
FFAP-200	70	TRIDECANE	8.62	0.0029	6.1209E-04	2.2879E-03	6.7853E-08	0.21	1.79
	30	DODECANE	12.60	0.0087	6.4166E-04	8.0583E-03	1.4090E-08		6.42
FFAP-250	70	TRIDECANE	7.87	0.0040	6.0367E-04	3.3963E-03	4.9087E-08	0.25	1.30
	30	DODECANE	12.70	0.0098	6.4219E-04	9.1578E-03	1.2315E-08		5.61

are shown in **Figure 7** and the same conclusions were drawn.

Efficiency was measured over the temperature range of interest to observe the impact of the phase change. **Figures 8a** and **8b** show efficiency for alkanes on SOX and the autocross-linkable PEG's as number of plates per meter, N/m, plotted against temperature. All curves exhibit a tremendous efficiency increase over a small temperature range which corresponds to the phase transition range in the DSC data if the lag time is taken into account. The dramatic efficiency increase reflects the difference between a separation based on adsorption and one based on partitioning.

The two uncross-linked columns, NXL and SOX, show an efficiency "crossover" going from low to high temperatures -- that is they show very poor efficiency in the adsorption mode, yet in the partitioning mode they possess higher efficiencies relative to the cross-linked columns. These observations are consistent with the behavior seen above for the HETP versus u curves.

The "dips" or discontinuities seen around 45°C for some of the curves are due to nonequilibration of the stationary phase, and is a factor of the time of injection after the

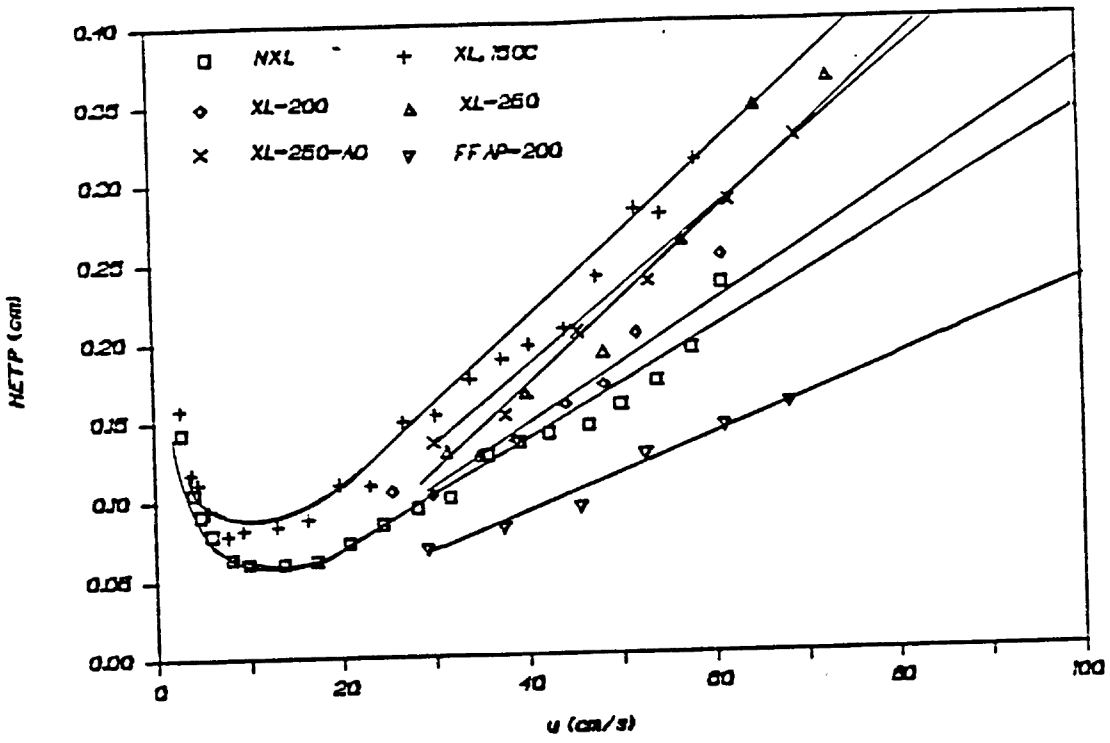

Figure 7. HETP v. u curves for PEG phase columns at 70°C with nitrogen carrier gas. Analyte = butanol.

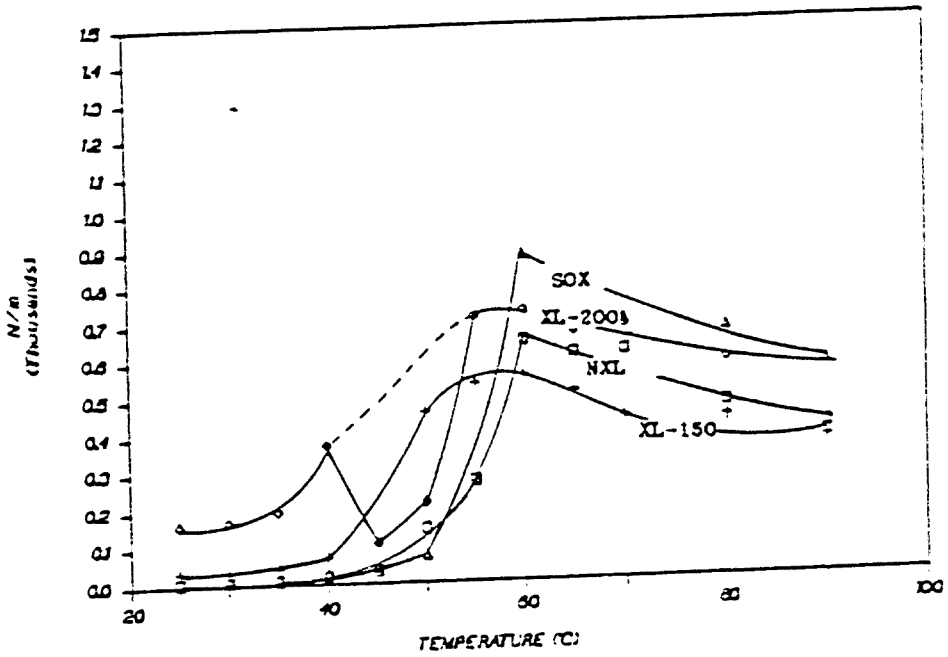

Figure 8a. N/m v. Temperature curves for the uncrosslinked columns (NXL and SOX) using nitrogen carrier gas. Comparison is made to two crosslinked columns (XL-150 and XL-200). Analyte = undecane

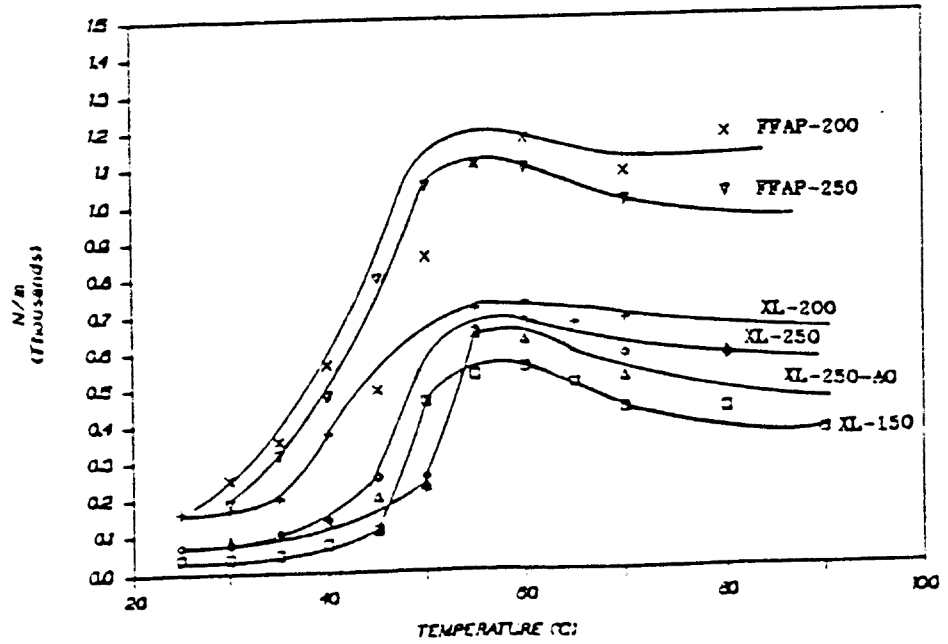

Figure 8b. N/m v. Temperature curves for the crosslinked PEG columns using nitrogen carrier gas. Analyte = undecane

column has reached the desired temperature and not the result of differences in the stationary phases. This phenomenon can be explained by a time lag due to crystallization. Approximately 60-70% of the PEG polymer exists as small, highly ordered crystallites which together form larger crystalline structures called spherulites. The remaining 30-40% of the polymer exists in an unordered, amorphous state. The high melting point and relatively low glass transition temperature, compared to other polyethers, are a direct result of this high degree of crystallinity.

In most cases, PEG crystallizes from its liquid state in two stages. Nucleation occurs first, followed by growth of these nuclei to form macroscopic spherulites. The crystallization half-times can be anywhere from ten minutes at 50°C, for a PEG of MW = 8000, to eighty minutes at 58°C for a PEG of MW = 20,000. During the crystallization time, the observed melting point is not very defined; it can vary a few degrees depending on the completeness of the crystallization and the equilibration of the polymer.

If cooled quickly, the polymer is not in a continuous state of equilibrium and crystallization is incomplete; as a result, the phase is in a highly amorphous state. The reverse is true if the polymer is heated quickly. At a

temperature the phase is assumed to be liquid, it actually still has some degree of crystallinity. The state of the phase greatly affects the chromatographic properties of the phase. In other words the polymer shows somewhat of a historesis when it is not thermally equilibrated at each point.

Figures 9a and **9b** show the analogous curves for an alcohol and exhibit much the same behavior as those for the alkane. All columns show an optimum efficiency at approximately 60°C. The only exception is the alcohol on NXL which gives a much earlier and narrower transition range, much lower optimum temperature (45°C), thus a lower minimum allowable operating temperature. A possible explanation is the better diffusion of an alcohol than an alkane in the more polar, uncross-linked polyethylene glycol stationary phase. In other words, the alcohol, which is capable of hydrogen bonding, is more soluble in the polar liquid phase.

The efficiencies of the remaining columns were also studied as a function of temperature (**Figures 10a** and **10b**). Because these plots were constructed using columns of different dimensions under slightly different conditions, the shape of these curves should be the focus and not the

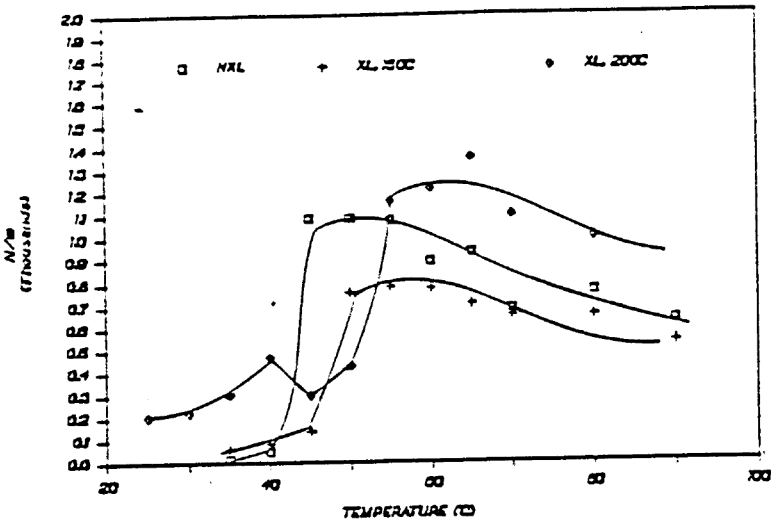

Figure 9a. N/m v. Temperature curves for the uncrosslinked NXL column using nitrogen carrier gas. Comparison is made to two crosslinked columns (XL-150 and XL-200). Analyte = butanol

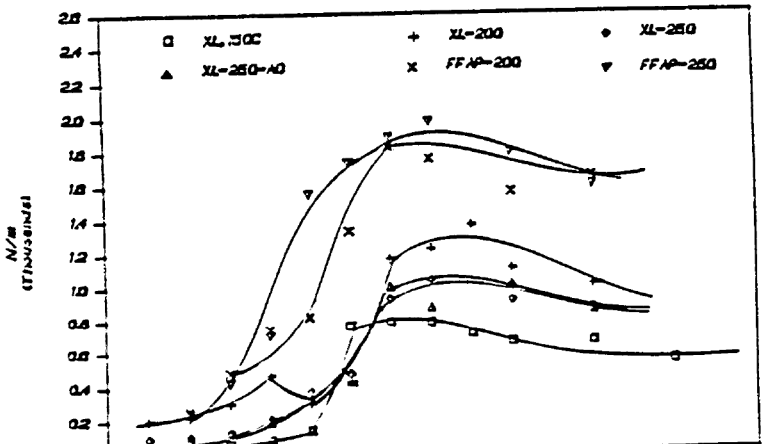

Figure 9b. N/m v. Temperature curves for the crosslinked PEG columns using nitrogen carrier gas. Analyte = butanol

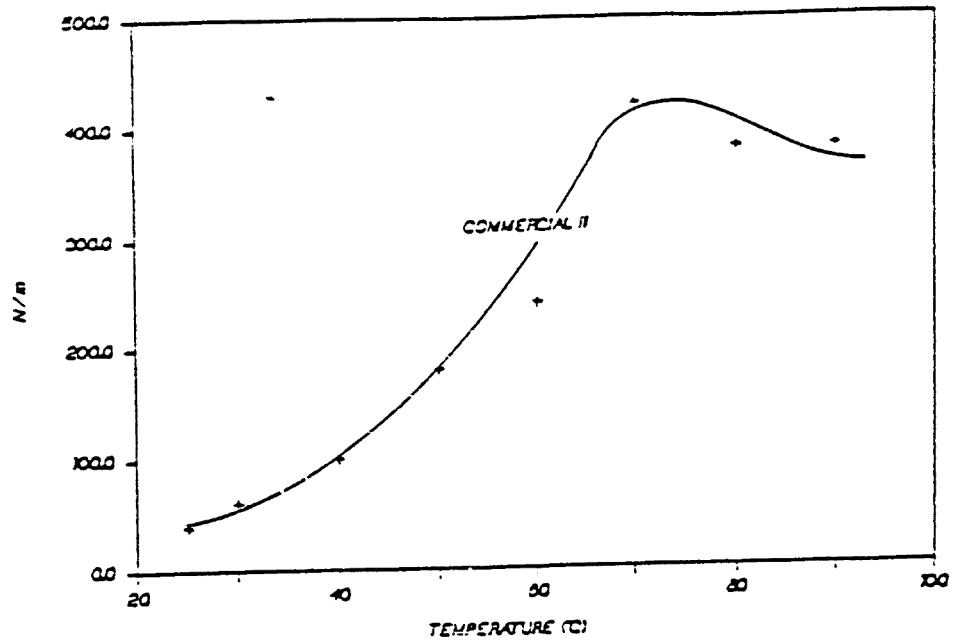

Figure 10a. N/m v. Temperature curve for the Commercial-II column using nitrogen carrier gas.

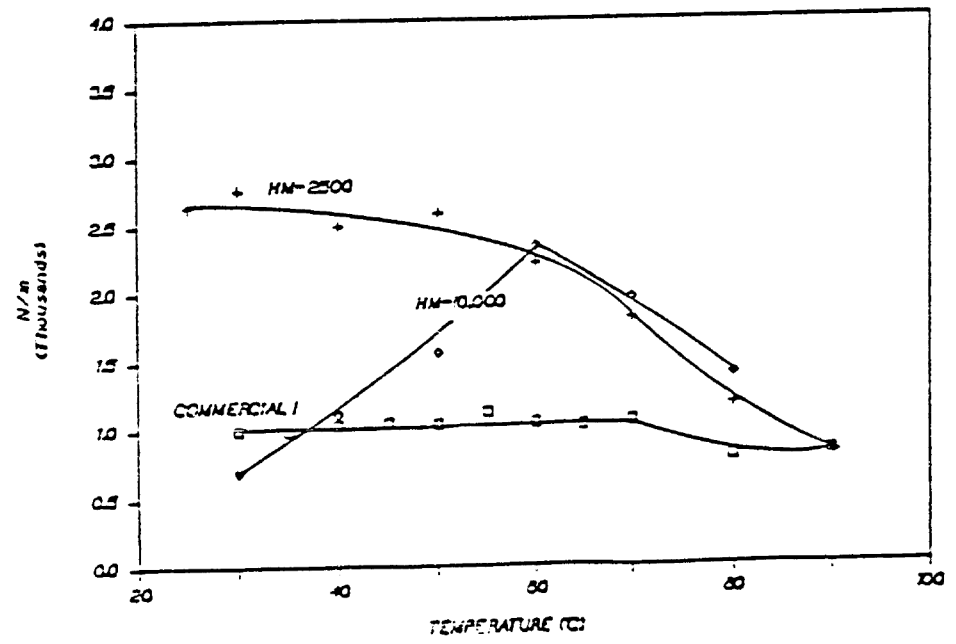

Figure 10b. N/m v. Temperature curve for the Commercial-I, HM-2500, and HM-10,000 columns. Nitrogen carrier gas was used for the two HM columns and hydrogen was used for Commercial-I.

exact plotted values. The Commercial-II column, **Figure 10a**, shows the same behavior as the columns in **Figure 8**. However in **Figure 10b**, only the curve for the HM-10,000 shows the same efficiency increase with temperature, and the maximum at 60°C corresponds with the maxima in **Figure 8**. The HM-2500 column, on the other hand, has no visible transition range. The transition probably occurs at a lower temperature due to the lower melting point of the lower molecular weight polymer. This is also the case for the Commercial-I column, for which efficiency is nearly independent of the temperature. The stationary phases used in the homemade columns were built up from lower molecular weight units than the stationary phase used for the Commercial-II column. The homemade phases (HM-10,000 and HM-2500) also had different end groups for cross-linking agents than the cross-linkable phases. It is clear that the characteristics of these end groups and the cross-linking reaction will influence the solid-liquid transition point. Together with increased molecular weight, longer chains give more crystallinity to the phase.

Separation Number

Like efficiency, TZ depends on retention time and peak width (Equation 4); therefore it serves mainly to confirm

the conclusions drawn from the efficiency data. Trenzahl number, TZ, versus u curves were constructed to study how separation is affected by cross-linking temperature. **Figures 11a** and **11b** respectively show the separation of dodecane and tridecane and of 2-pentanol and 1-butanol on the cross-linked columns; the low separation numbers for the alcohols is because 2-pentanol and 1-butanol are not serial homologs. The order of increasing separation corresponds to the order of increasing efficiency listed above, thus confirming that 200°C is the optimum cross-linking temperature and the FFAP phase possesses higher efficiency and separation than the autocross-linkable PEG phases.

To observe the impact of the phase change on separation, TZ was plotted versus temperature. **Figures 12a** and **12b** show the separation of decane and undecane, and **Figures 13a** and **13b** show the separation of propanol and butanol. As in the efficiency versus temperature curves, the same large transition going from low to high temperatures is observed for all columns, and the order of increasing separation corresponds to the order of increasing efficiency as above. Again, the only difference

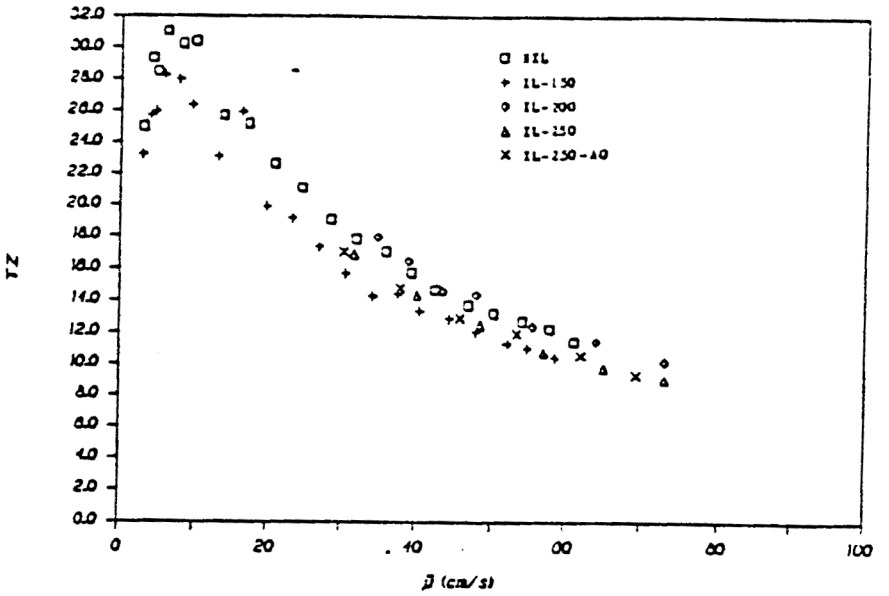

Figure 11a. TZ v. u curves for separation of n-dodecane and n-tridecane on the autocross-linkable PEG phases using nitrogen carrier gas at 70°C.

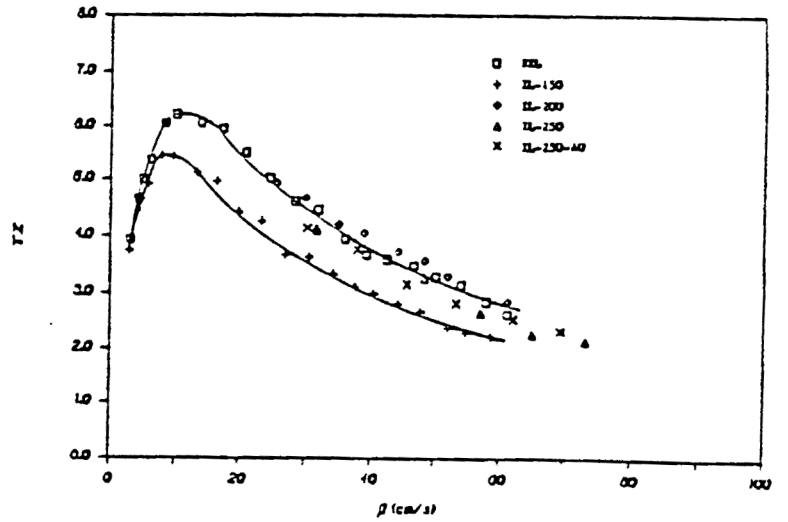

Figure 11b. TZ v. u curves for separation of 2-pentanol and 1-butanol on the autocross-linkable PEG phases using nitrogen carrier gas at 70°C.

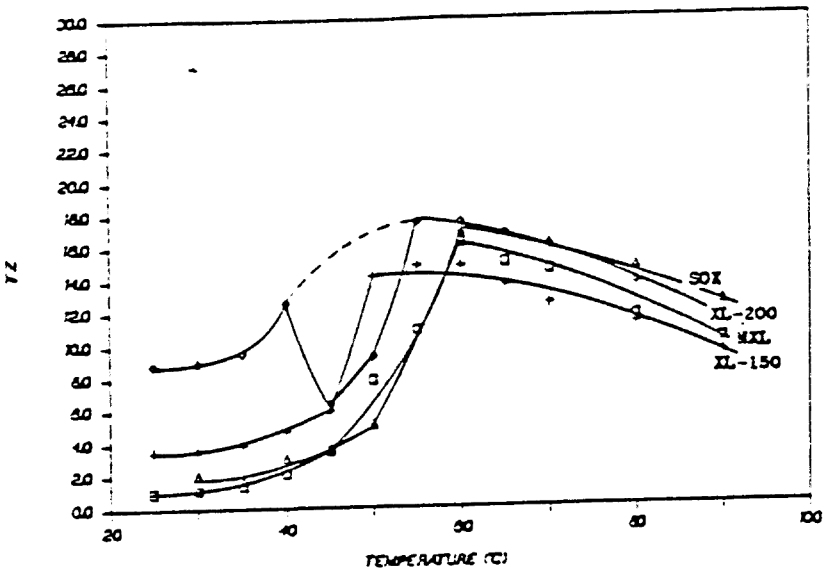

Figure 12a. TZ v. Temperature curves for the uncrosslinked columns (NXL and SOX) using nitrogen carrier gas. Comparison is made to two crosslinked columns (XL-150 and XL-200). Analytes = decane and undecane

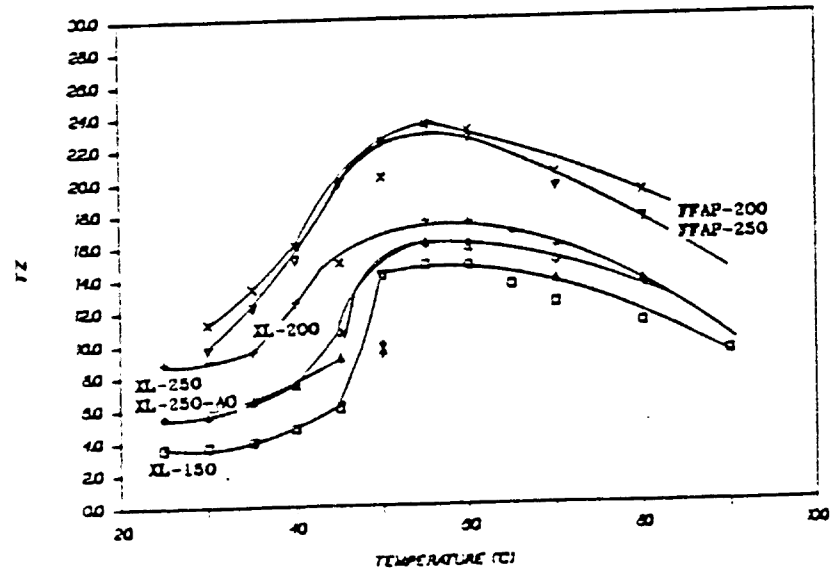

Figure 12b. TZ v. Temperature curves for the crosslinked PEG columns using nitrogen carrier gas. Analytes = decane and undecane.

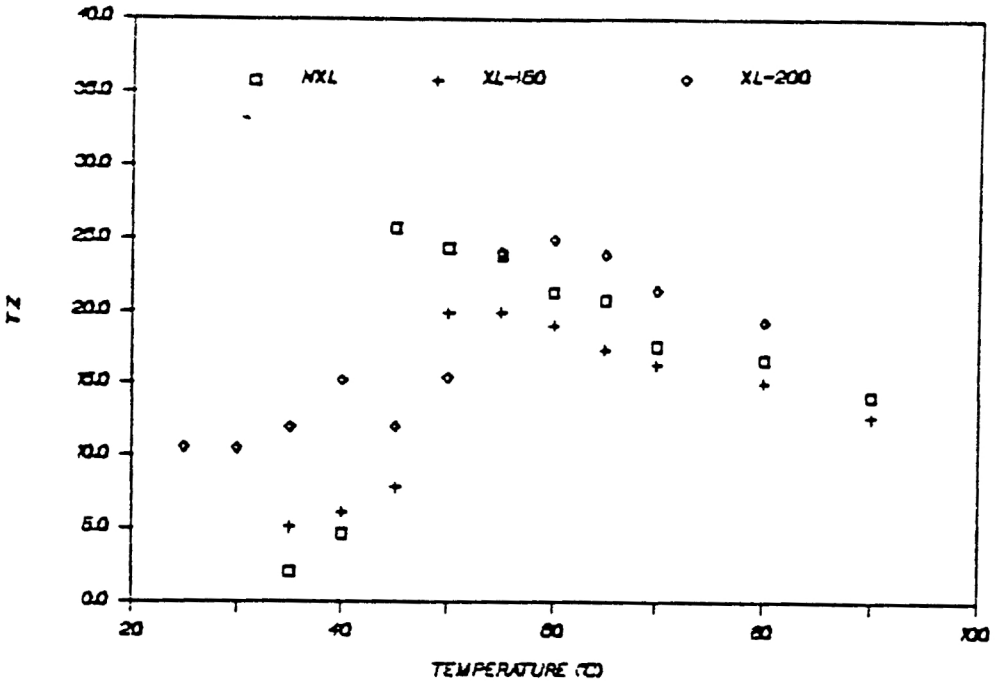

Figure 13a. TZ v. Temperature curves for the uncrosslinked NXL column using nitrogen carrier gas. Comparison is made to two crosslinked columns (XL-150 and XL-200). Analytes = propanol and butanol

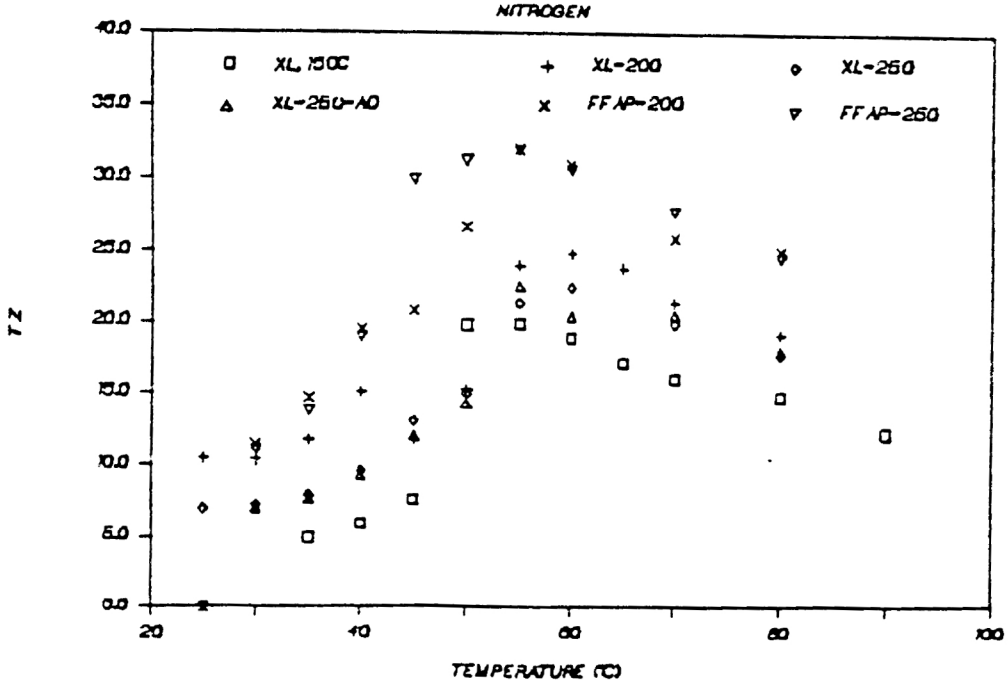

Figure 13b. TZ v. Temperature curves for the crosslinked PEG columns using nitrogen carrier gas. Analytes = propanol and butanol.

observed between the alkanes and alcohols is the earlier, more narrow transition for the alcohols on the NXL column. The efficiency and TZ versus u curves are proven similar as are the efficiency and TZ versus T curves. Therefore all of the relevant conclusions drawn above for the efficiency curves apply to and are confirmed by the separation curves.

Capacity

Because capacity is mainly a function of the solubility of the analyte in the stationary phase, it does not vary appreciably with carrier gas velocity. Therefore, only k versus T curves were constructed. The temperature dependence of the capacity factor of alkanes is seen in **Figures 14a, 14b** and **14c.** There is a decrease in capacity ratio with increasing column temperature: k decreases as solute volatility increases. **Figures 14a** and **14b**, plotted for the commercial 20,000 MW PEG phases, possess an obvious discontinuity. As the solid-liquid phase transition is approached, retention is suddenly enhanced due to the dramatically increased solvent properties of the liquid phase. The autocross-linkable phases all have their capacity increase between 40°C and 50°C, whereas the SOX

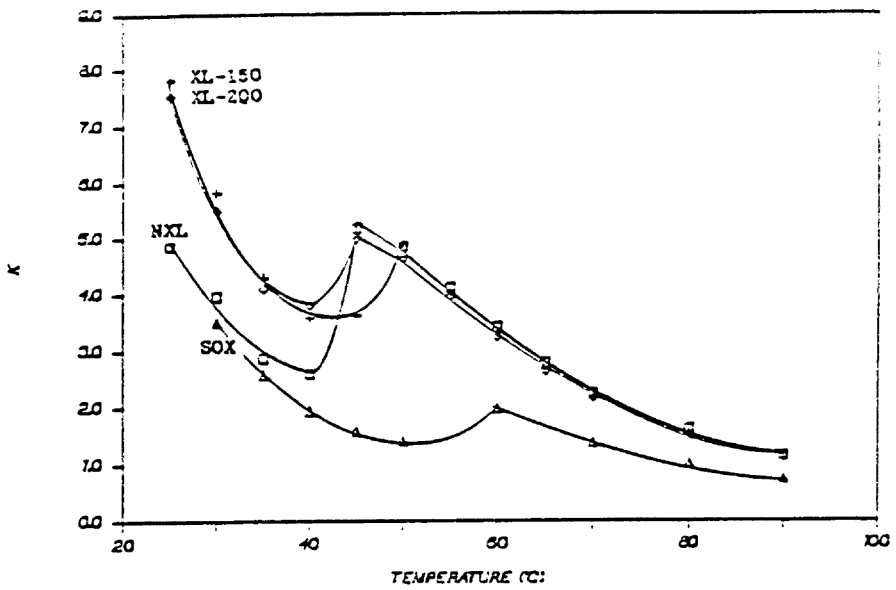

Figure 14a. k v. Temperature curves for the uncrosslinked columns (NXL and SOX) using nitrogen carrier gas. Comparison is made to two crosslinked columns (XL-150 and XL-200). Analyte = undecane

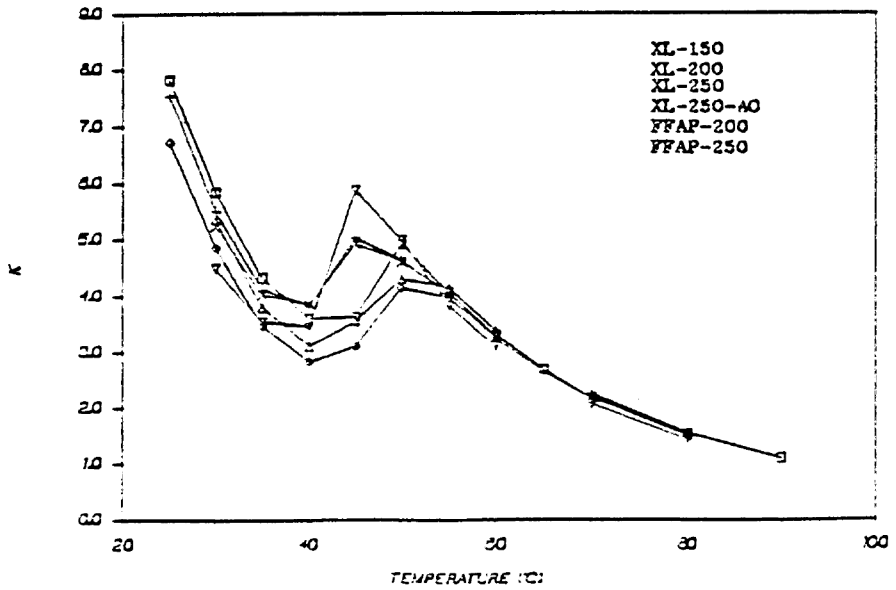

Figure 14b. k v. Temperature curves for the crosslinked PEG columns using nitrogen carrier gas. Analyte = undecane

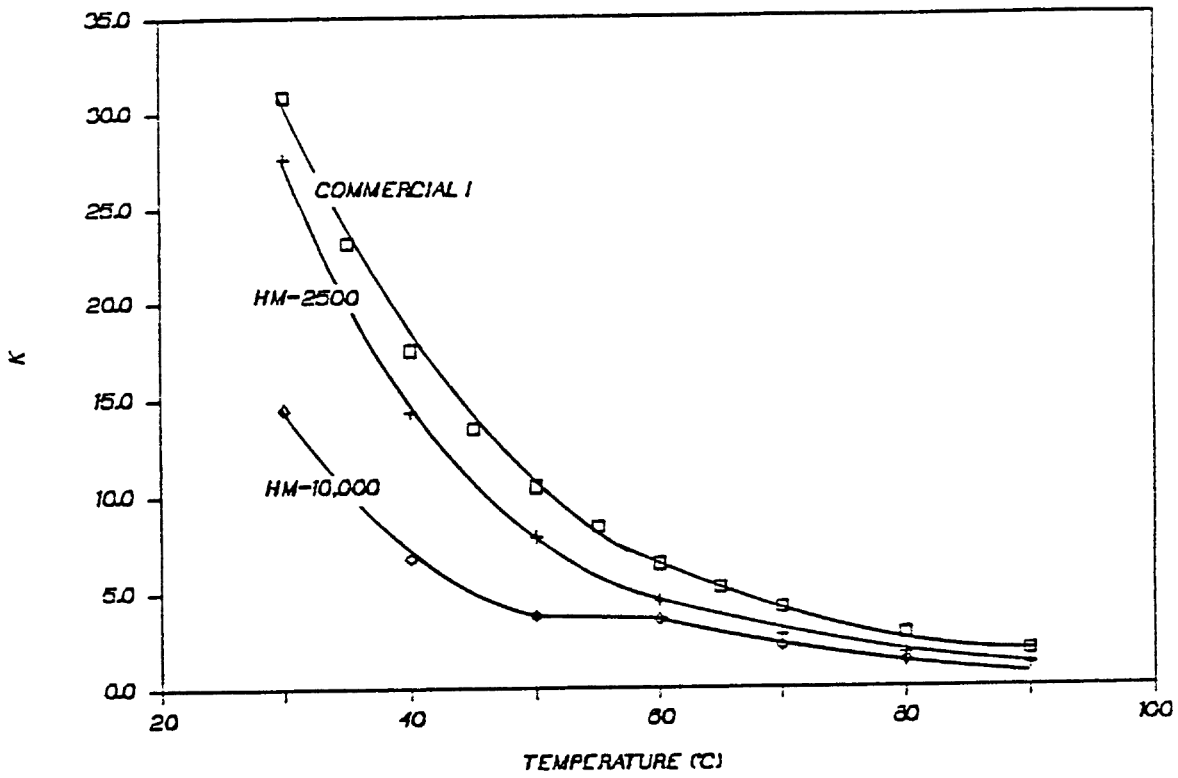

Figure 14c. k v. Temperature curve for the Commercial-I, HM-2500, and HM-10,000 columns. Nitrogen carrier gas was used for the two HM columns and hydrogen was used for Commercial-I.

phase does not begin this increase until after 50°C. After a certain point, the volatility increase again becomes more important, and the retention decreases with temperature. A comparable behavior has been reported by Janini et al.[27] for liquid crystal stationary phases over the smectic-nematic phase transition.

The curves in **Figure 14c** do not show this effect. Only the HM-10,000 phase displays a levelling between 50°C and 60°C. For the HM-2500, an exponential decrease is noted. The similarity in the two columns, Commercial-I and HM-2500, noted in the N/m versus T curves is thereby confirmed.

Crystallization Delay Time

The theory of a delay time (historesis) derived from the DSC scan is chromatographically demonstrated in **Figure 15.** The XL-250 column was used for this demonstration, but this is unimportant since any of the PEG phases of MW=20,000 would exhibit this behavior. The column was held at 70°C for one hour and then cooled to 30°C. A series of injections of alkanes was begun thirty minutes later (t_i) at 30°C. Both efficiency and capacity declined for a considerable time. Since t_i was approximately thirty minutes after reaching 30C, the intense initial

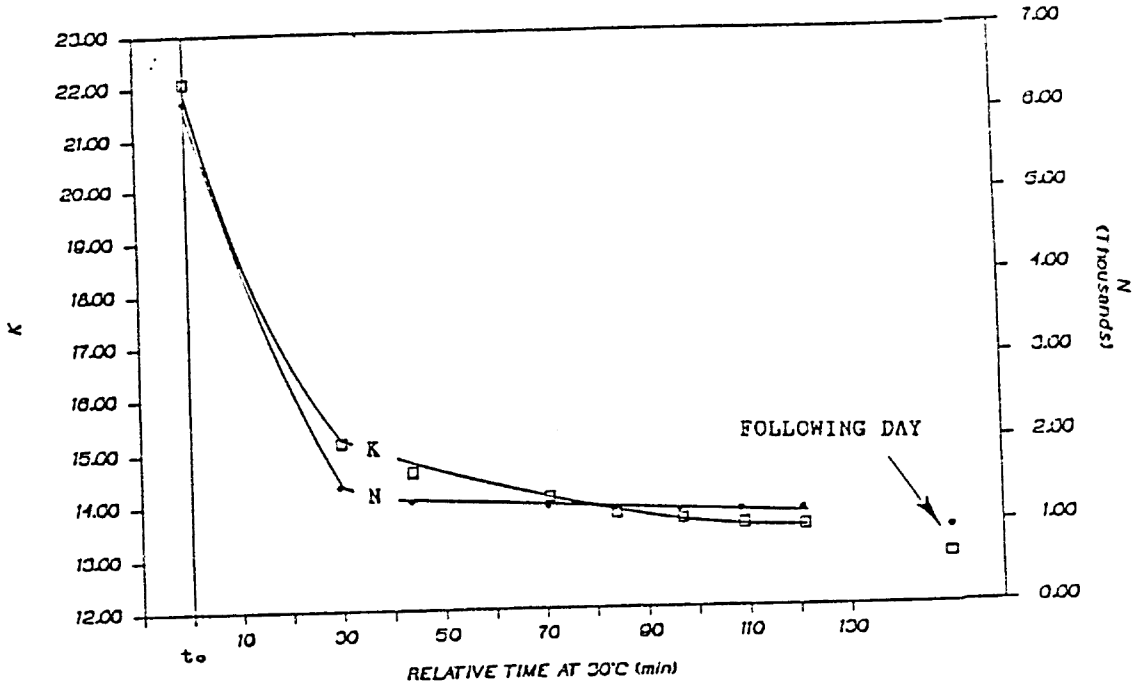

Figure 15. k and N v. Time at 30°C.

decrease occurred during the first hour, then levelled, but was still diminishing ninety minutes later. The following day still slightly lower efficiency and capacity were measured. This indicates a very slow thermal equilibrium to the final crystal structure.

Some manufacturers advertise their PEG columns as having a minimum operating temperature of 50° or 60°C. If used at or below its minimum temperature a retention time shift may occur as well as a change in efficiency, depending on the equilibration time at this temperature. This phenomenon can cause serious problems in the laboratory, as seen in **Figure 16**. All of the analyses were run on the XL-250-AO column under identical conditions: 1uL injection of C_9 - C_{12} n-hydrocarbons (1ug/uL in hexane), split ratio 1:100, hydrogen carrier gas (u=33cm/s), 45°C isothermal. As above, choice of column was unimportant. The first chromatogram, is one of five run after heating the column to 45°C after standing at 27°C for twenty-four hours. The retention times, plate count and capacity remained nearly constant over the two hour period. Capacity and plate count are given for the last peak, C_{12}, in each chromatogram.

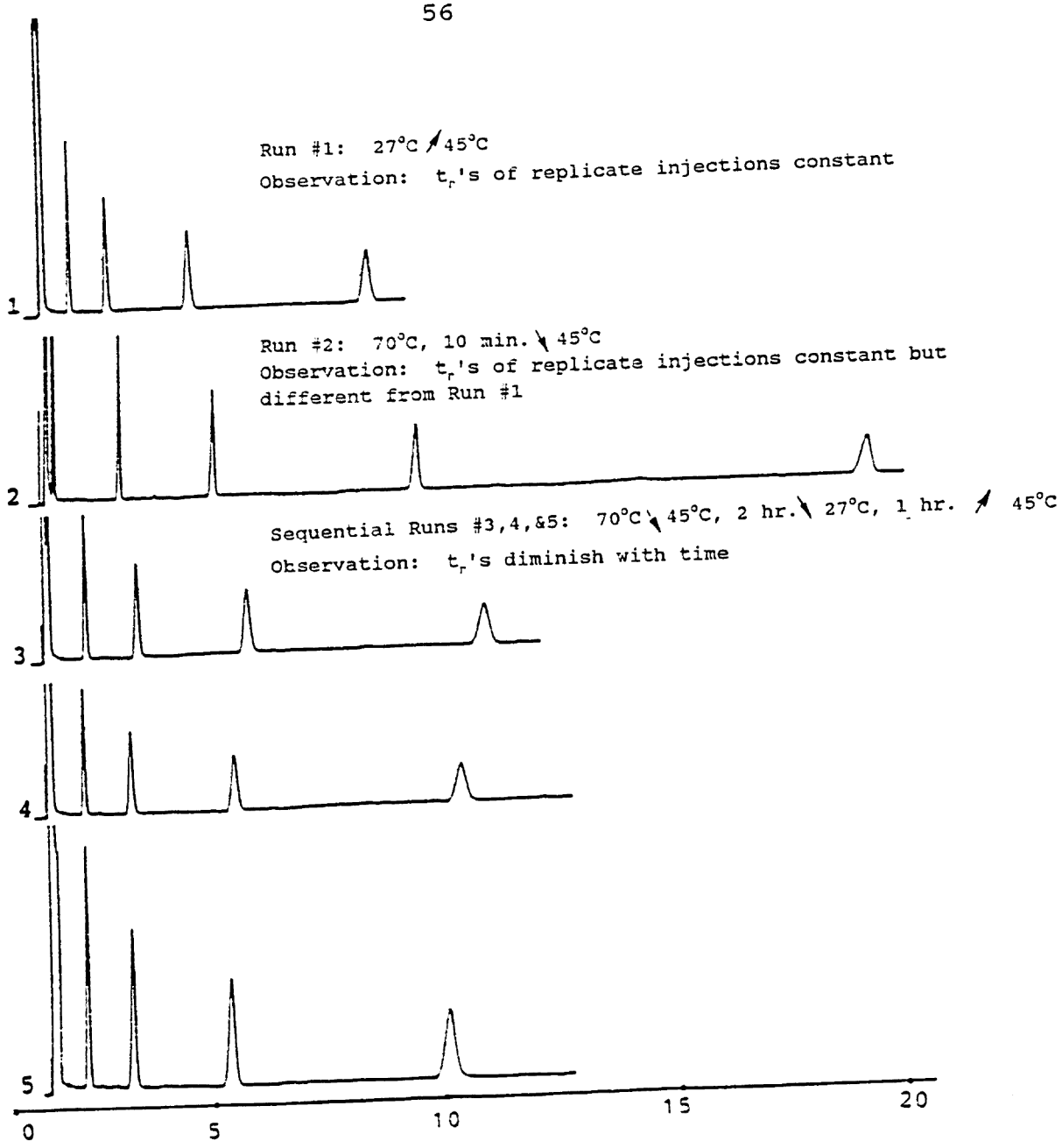

Figure 16. Five chromatographic analyses of C_9-C_{12} hydrocarbons under identical conditions (hydrogen carrier gas at u=33 cm/s, 45°C isothermal.

The column was then heated to 70°C and held for ten minutes and then cooled back to 45°C. Five more chromatograms were run; again retention time, plate count and capacity remained nearly constant for the three hour analysis period, yet these values were very different from the previous values. The second chromatogram is representative of these five.

Finally the column was cooled again to 27°C for one hour and the reheated to 45°C. The third chromatogram was run immediately upon reaching 45°C; the fourth, forty-two minutes later; and the fifth, 128 minutes later. Retention time, capacity and plate number continued to decrease over this three hour period.

This practical demonstration of the crystallization delay time illustrates one of the problems with PEG phases, while also giving a better understanding to the "dips" in the N/m and TZ versus T curves.

Selectivity

Finally a look at the retention indices tells us something about the polarity and selectivity of the different phases. **Figure 17a** and **17b** show the retention behavior of propanol with respect to the hydrocarbons as a

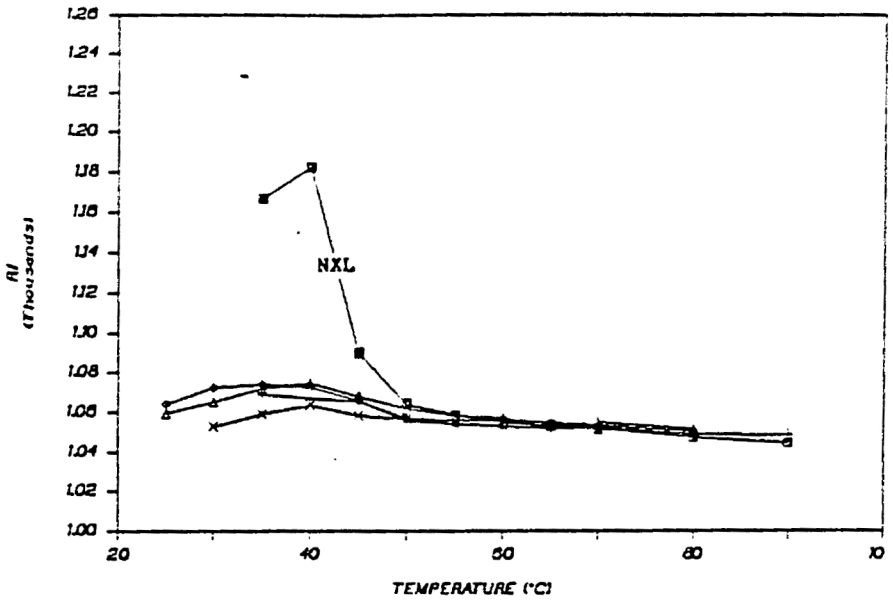

Figure 17a. RI v. Temperature curves for propanol on the autocrosslinkable PEG phases using nitrogen carrier gas.

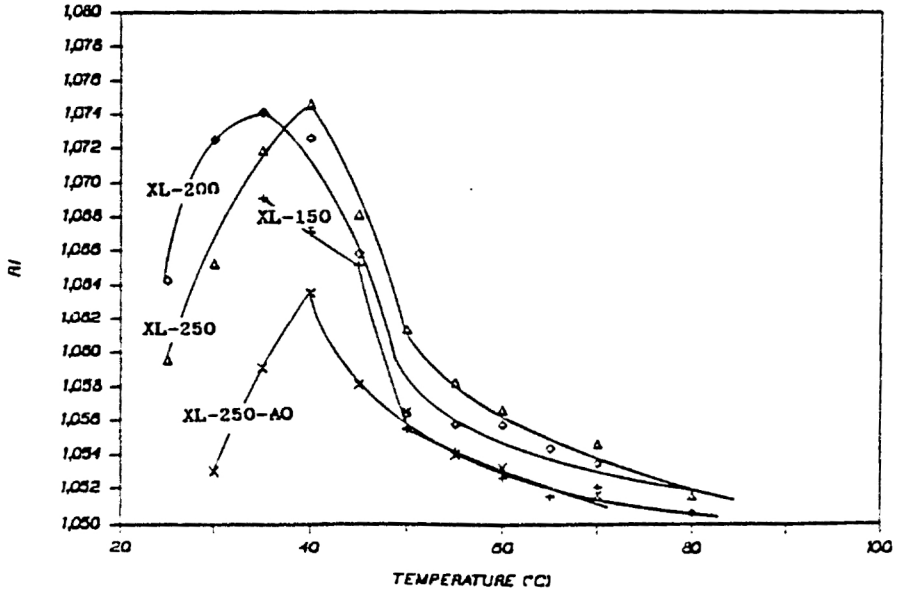

Figure 17b. RI v. Temperature curves for propanol on the crosslinked PEG and FFAP phases using nitrogen carrier gas. Note scale.

function of temperature. The alcohol shows best retention on the more polar uncross-linked phase at low temperatures due to the high degree of hydrogen bonding as seen in **Figure 17a.** The maximum RI occurs not in the strict adsorption mode, but at the transition between the solid and liquid phases at 40°C; at this point, the alcohol benefits from both increased partitioning and polarity of the phase. At higher temperatures the volatility of the alcohols overcomes this enhanced retention and the difference between the uncross-linked and cross-linked phase is minimal. This same effect was seen in the capacity ratio curves (**Figure 14**). In **Figure 17b**, which shows an enlarged portion of **Figure 17a**, the cross-linked phases do not show as much change with temperature -- the added hydrogen bonding of the reactive end groups is lost upon immobilization, although the polarity of the phase increases with increasing cross-linking temperature. Also, the maximum RI occurs approximately 5°C earlier on XL-150 and XL-200 than on NXL.

XL-200 and XL-250 show the greatest maximum retention among the cross-linked columns. The addition of the antioxidant to the phase also decreases its polarity -- there is approximately a difference of ten RI units between the maximum RI of XL-250 and XL-250-AO.

The retention indices of a wider range of compounds were used to further investigate the impact of carrier gas, column cross-linking temperature, and column operating temperature on the polarity of the phase. The RI values for each analysis are tabulated in **Table 4.** The McReynolds compounds were analyzed at 30°C and 70°C on NXL and XL-150 using hydrogen, nitrogen, and carbon dioxide as carrier gas. The retention indices are compared in bar graphs in **Figure 18** (see Table 4 for abbreviated compound names). In nearly every case, at 30°C and 70°C, nitrogen gives the highest retention. The greatest variance in RI due to carrier gas is seen in the adsorption mode on NXL (**Figure 18a**); the influence of carrier gas is minimal on NXL in the partitioning mode (**Figure 18b**) and for XL-150 in both modes.

Figures 19a, 19b, 19c and **19d** show the influence of column operating temperature and cross-linking temperature. At 30°C, NXL gives the highest overall retention, again due to its heightened polarity from the unreacted cross-linking agent. Commercial-I exhibits the second highest retention, but is more likely due to its enhanced partitioning at low temperatures observed in the N/m versus T curve (**Figure 9d**).

Table 4. Retention Indices of McReynolds Compounds on Various Columns.

COMPOUND		Column-- COMM I Car. Gas H2 Temp.--- 30C	COMM I H2 70C	NXL H2 30C	NXL H2 70C	NXL N2 30C	NXL N2 70C	NXL CO2 30C	NXL CO2 70C
BENZENE	BEN	945.2	961.5	926.6	954.5	934.4	955.6	927.0	955.7
1-IODOBUTANE	BUT	1053.8	1067.3	1038.0	1073.0	1049.3	1074.7	1039.1	1073.5
2-OCTYNE	OCT	1063.9	1055.3	1050.6	1062.9	1051.5	1063.9	1039.9	1063.5
1,4-DIOXANE	DIO	1062.3	1067.3	1051.4	1073.0	1056.6	1074.7	1044.1	1073.5
CIS-HYDRINDANE	HYD	1085.8	1083.1	1081.5	1115.4	1084.3	1116.2	1076.0	1116.4
BUTANOL	4OL	1159.2	1143.9	1188.6	1158.2	1193.2	1160.2	1192.1	1159.9
PYRIDINE	PYR	1178.3	1200.0	1174.4	1190.7	1178.3	1192.5	1177.3	1191.6
NITROPROPANE	NIPR	1203.6	1218.6	1179.2	1216.1	1183.2	1218.3	1180.6	1217.3
2-METHYL-2-PENTANOL	5OL	1117.9	1089.4	1158.7	1115.4	1172.7	1116.2	1161.2	1116.4
	SUM	9870.0	9886.4	9849.0	9959.2	9903.5	9972.4	9837.1	9968.0

COMPOUND		Column-- XL-150 Car. Gas H2 Temp.--- 30C	XL-150 H2 70C	XL-150 N2 30C	XL-150 N2 70C	XL-150 CO2 30C	XL-150 CO2 70C	XL-200 N2 30C	XL-200 N2 70C
BENZENE	BEN	936.1	958.3	936.7	958.3	933.4	956.8	947.6	966.0
1-IODOBUTANE	BUT	1041.3	1074.4	1044.7	1075.9	1042.3	1074.3	1041.2	1080.9
2-OCTYNE	OCT	1046.6	1064.1	1045.4	1064.8	1045.1	1064.2	1046.2	1068.3
1,4-DIOXANE	DIO	1053.2	1074.4	1054.0	1075.9	1052.7	1074.3	1061.2	1080.9
CIS-HYDRINDANE	HYD	1077.7	1115.6	1079.5	1115.9	1079.2	1116.2	1068.0	1118.7
BUTANOL	4OL	1185.3	1158.6	1185.1	1159.7	1186.0	1159.4	1163.2	1160.8
PYRIDINE	PYR	1176.8	1191.6	1176.9	1192.5	1176.0	1191.5	1176.4	1200.0
NITROPROPANE	NIPR	1190.3	1219.9	1192.4	1221.0	1192.4	1220.2	1196.5	1229.7
2-METHYL-2-PENTANOL	5OL	1151.5	1115.6	1151.5	1115.9	1150.6	1116.2	1118.4	1110.9
	SUM	9858.7	9972.4	9866.2	9979.8	9857.7	9973.3	9818.7	10016.2

Table 4. Continued

COMPOUND		XL-250 N2 30C	XL-250 N2 70C	XL-250-A N2 30C	XL-250-A N2 70C	SOX N2 30C	SOX N2 70C
BENZENE	BEN	944.2	969.0	934.0	966.7	1000.0	955.7
1-IODOBUTANE	BUT	1041.2	1083.0	1031.2	1080.6	996.4	1072.0
2-OCTYNE	OCT	1043.1	1070.3	1036.8	1068.1	1055.4	1063.9
1,4-DIOXANE	DIO	1055.1	1087.0	1049.3	1083.3	1000.0	1069.5
CIS-HYDRINDANE	HYD	1065.6	1119.8	1059.1	1118.0	1017.3	1112.1
BUTANOL	4OL	1162.7	1163.0	1149.2	1158.7	1101.0	1140.7
PYRIDINE	PYR	1175.3	1202.9	1162.2	1198.5	1136.0	1189.3
NITROPROPANE	NIPR	1192.8	1232.4	1177.8	1227.6	1124.9	1215.3
2-METHYL-2-PENTANOL	5OL	1119.3	1113.3	1107.2	1109.7	1056.2	1093.3
		9799.3	10040.6	9706.8	10011.2	9487.2	9911.9

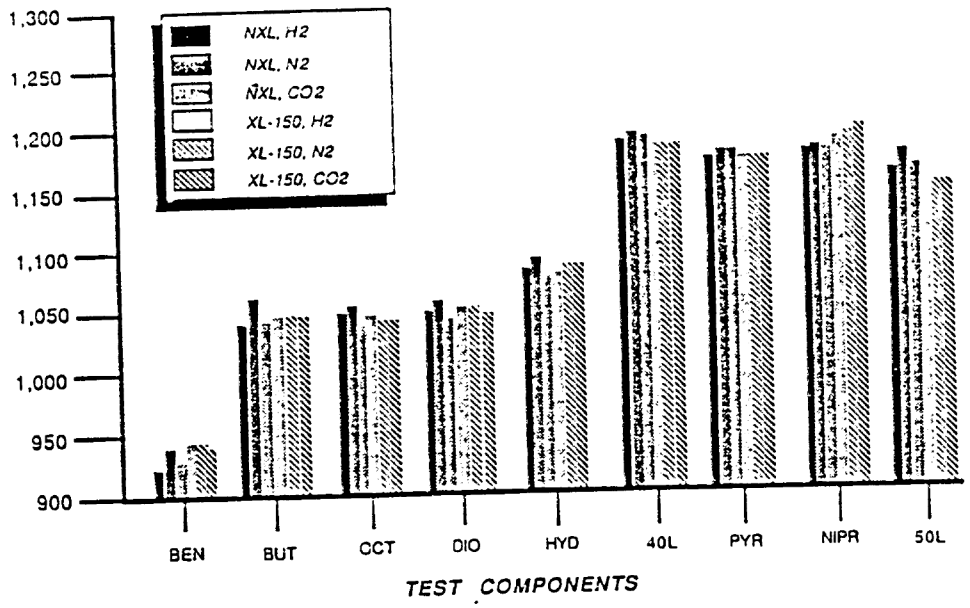

Figure 18a. Retention indicies of McReynolds compounds at 30°C using hydrogen, nitrogen, and carbon dioxide as carrier gas.

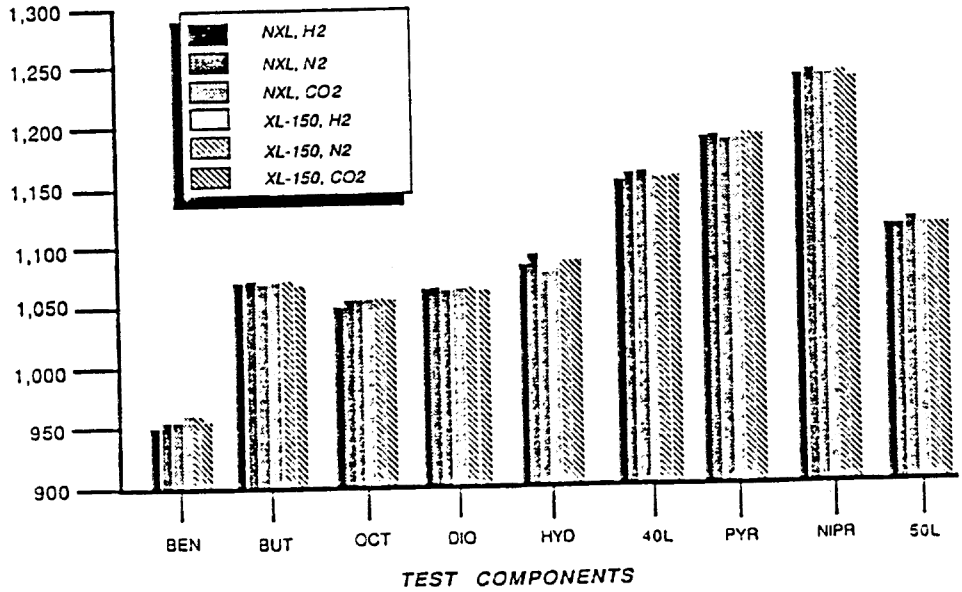

Figure 18b. Retention indices of McReynolds compounds at 70°C using hydrogen, nitrogen, and carbon dioxide as carrier gas.

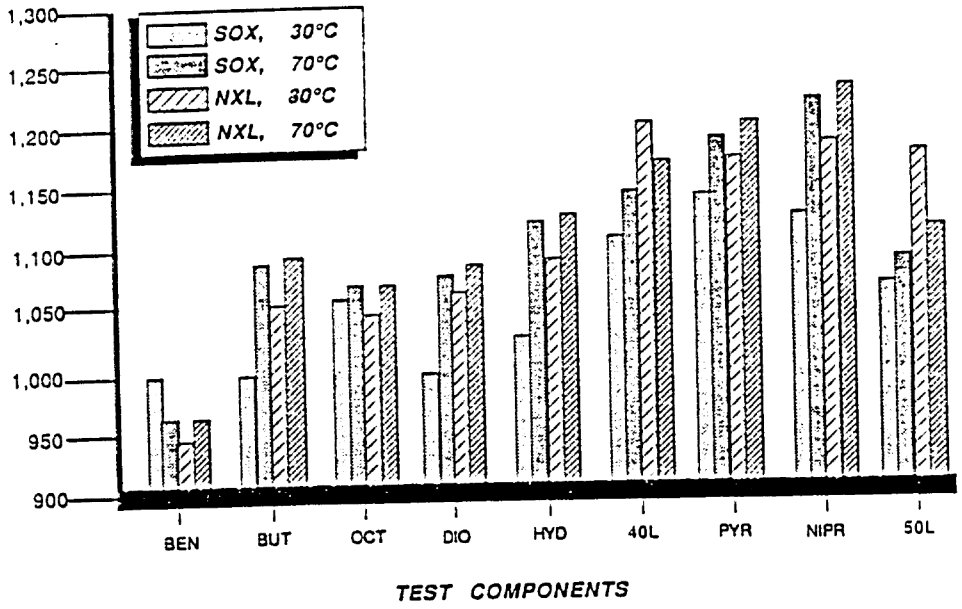

Figure 19a. Retention indices of McReynolds compounds at 30°C and 70°C on NXL and SOX columns using nitrogen as carrier gas.

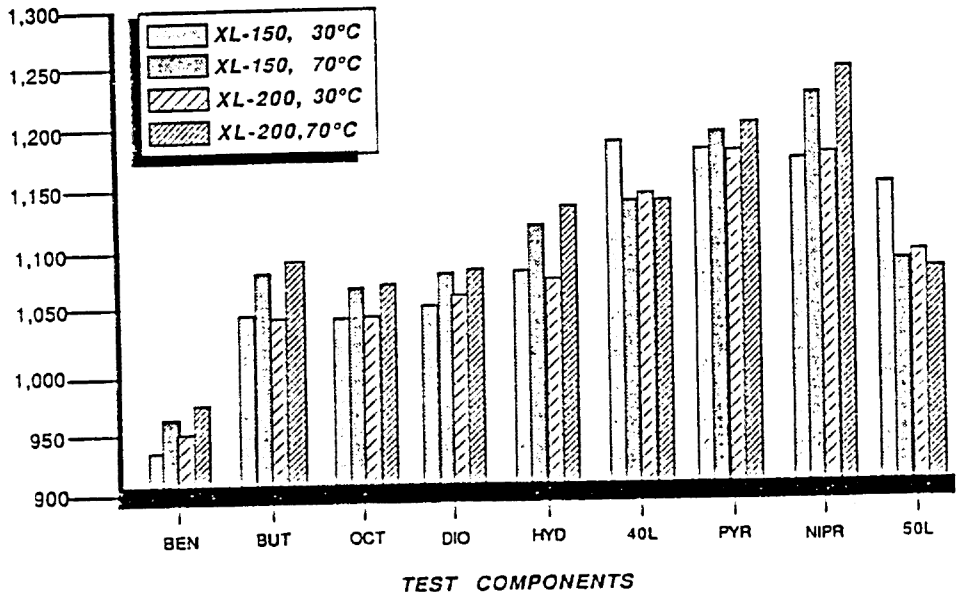

Figure 19b. Retention indices of McReynolds compounds at 30°C and 70°C on XL-150 and XL-200 columns using nitrogen as carrier gas.

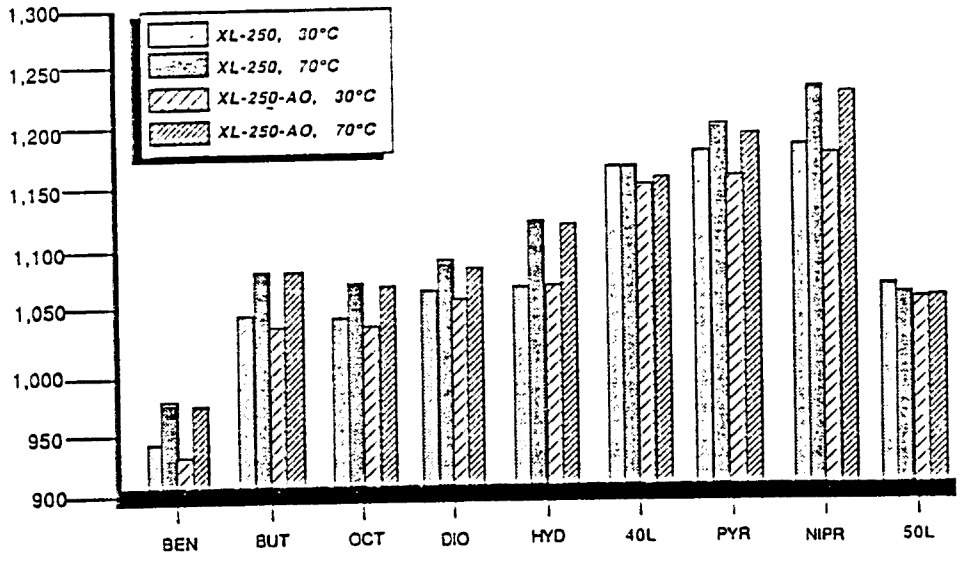

Figure 19c. Retention indices of McReynolds compounds at 30°C and 70°C on XL-250 and XL-250-AO columns using nitrogen as carrier gas.

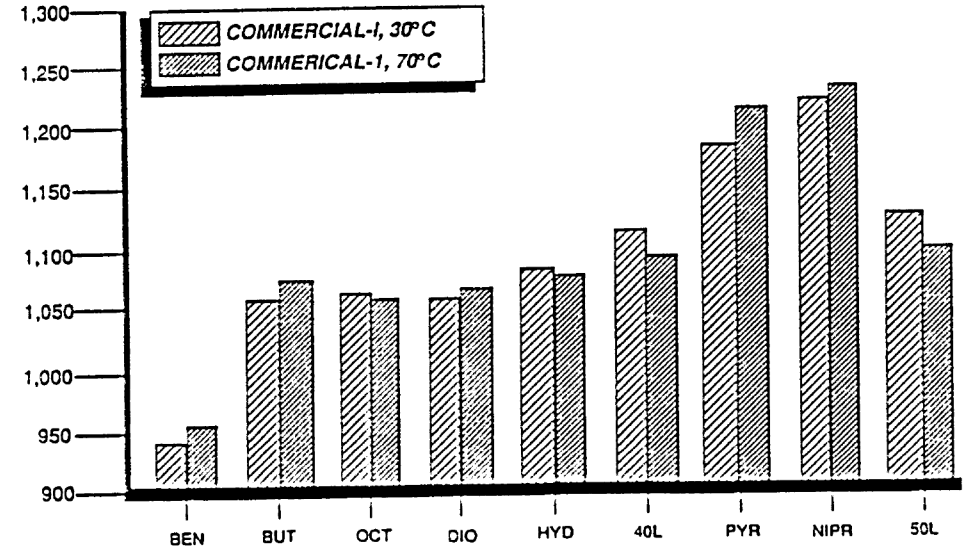

Figure 19d. Retention indices of McReynolds compounds at 30°C and 70°C on Commercial-I using hydrogen as carrier gas.

In the adsorption mode the overall retention indices of the cross-linked columns decreases with increasing cross-linking temperature, and SOX shows the lowest overall retention. In the partitioning mode, the order of overall retention is nearly the reverse; among the autocross-linkable columns retention increases with increasing cross-linking temperature. SOX and Commercial-I display the lowest overall retention. In both modes, the addition of antioxidant causes decreased retention.

In nearly all cases, overall retention is higher at 70°C than at 30°C. With the exception of SOX and XL-250-AO, the alcohols exhibit increased retention in the adsorption mode. In agreement with **Figure 17a**, NXL shows the highest retention of the alcohol at low temperatures. The important role of hydrogen bonding is best seen in comparing the RI of butanol and 2-methyl-2-pentanol; though the butanol has a lower molecular weight, it is better retained because of its better hydrogen bonding capability. The geminal methyl group causes the hydroxy group on the pentanol to be more sterically hindered, resulting in decreased hydrogen bond strength. This small amount of steric hindrance causes a large difference in retention time.

CONCLUSION

In this study, the behavior of polyethylene glycol liquid phases were investigated, especially their chromatographic behavior at low temperatures and the dependence of efficiency, retention, and separation on cross-linking conditions. Three main conclusions were drawn. First, efficiency is strongly dependent on cross-linking conditions; above the solid-liquid transition temperature, NXL is better than XL-150, yet XL-250 and XL-200 are better than NXL, XL-200 being the better of the two. The uncross-linked, pure PEG column, SOX, showed the best overall efficiency.

Second, the retention behavior differs greatly between the adsorption and partitioning mode. For cross-linked columns, most compounds, with the exception of alcohols, show increased retention in the partitioning mode. The transition point between the two modes is dependent on the degree of crystallinity of the phase which is influenced by the degree of cross-linking, the end groups, and the molecular weight of the PEG units from which the phase is constructed.

Finally, the retention index of the phase is strongly dependent on: 1) the operating temperature (30°C versus

70°C), 2) the cross-linking conditions, and 3) the end groups and cross-linking agents present in the phase.

REFERENCES

[1] M. Golay, Gas Chromatograpy 1958, D.H. Desty, ed., Butterworths, London, 1959, p. 36.

[2] M. Proot, F. David, P. Sandra, and M. Verzele, HRC & CC 1985, 8, 426.

[3] P. Sandra, F. David, M. Proot, G. Diricks, M. Verstappe, and M. Verzele, HRC & CC 1985, 8, 782.

[4] T.J. Stark, P.A. Larson, and R.D. Dandeneau, J. Chromatogr. 1983, 279, 31.

[5] I. Temmerman, PhD thesis, University of Ghent, Belgium, 1984.

[6] M. Verzele and P. Sandra, J. Chromatogr. 1978, 158, 111.

[7] P. Sandra, M. Verzele, M. Verstappe and J. Verzele, HRC & CC, 1979, 2 288.

[8] M. Godefroot, M. Van Roelenbosch, M. Verstappe, P. Sandra and M. Verzele, HRC & CC, 1980 3 337.

[9] K. Grob, G. Grob, and K. Grob, Jr., J. Chromatogr. 1978, 156, 1.

[10] G. Diricks, Ph.D. Thesis, University of Ghent, 1985.

[11] C.A. Cramers, C.E. Van Tilburg, C.P.M. Schutjes, J.A. Rijks, G.A. Rutten, and R. De Nijs, J. Chromatogr. 1983, 279, 83.

[12] C.R. Hastings and W.A. Aue, J. Chromatogr. 1974, 89, 369.

[13] D.A. Cronin, J. Chromatogr. 1974, 97, 263.

[14] L. Blomberg, J. Chromatogr. 1975 115, 365.

[15] G. Schomburg, H. Husmann and F. Weeke, J. Chromatogr. 1974, 99, 63.

[16] K. Grob and G. Grob, J. Chromatogr. 1976, 125, 471.

[17] N.F. Ives and L. Giuffrida, J. Assoc. Off. Anal. Chem. 1970, 53, 976.

[18] J.J. Franken, R.C.M. de Nijs and F.L. Schulting, J. Chromatogr. 1974, 144, 253.

[19] R. F. Arrendale, L.B. Smith and L.B. Rogers, HRC & CC 3 (1980) 115.

[20] P. Sandra, M. Van Roelenbosch, I. Temmerman and G. Redant, Analysis of Organic Micropollutants in Water, Proceedings of the Sec. Eur. Symp., G. Angeletti and A. Bjorseth, ed., Killarney, 1981, p. 99.

[21] R.C.M. de Nijs and J. de Zeeuw, HRC & CC, 1982, 6, 501.

[22] J. Buyten, L. Blomberg, K. Markides and T. Wannman, J. Chromatogr. 1983, 268, 60.

[23] H. Traitler, HRC & CC 1983, 6, 60.

[24] H. Traitler and L. Kolarovic, Fifth Int. Symp. on Cap. Chromatography, Riva del Garda, J. Rijks, ed., Elsevier, 1983, p. 49.

[25] V. Martinez de la Gandara, J. Sanz and I. Martinez-Castro, HRC & CC 1984, 1, 44.

[26] P. Sandra, I. Temmerman, and M. Verstappe, HRC & CC 1983, 6, 501.

[27] G.M. Janini, G.M. Muschik, and W.L. Zielinski, Anal. Chem. 1976, 48, 809.

The vita has been removed from the scanned document